3.2.1 Landsat Data

3.2.1.1 Vassova lagoon

The points selected for Chl-a concentration extraction for the eutrophication assessment in Vassova lagoon, are shown in Figure 75. These points cover the typical conditions at all sub-basins of the lagoon and are distributed among various depths.

Figure 75. Points for Chl-a concentration extraction in Vassova lagoon.

Table 8 presents the statistical measures for Chl-a concentration at all points examined in Vassova lagoon.

Table 8. Statistical measures per point for Chl-a concentration at Vassova Lagoon.

Points	Min	Max	Median	Mean	St. deviation	Skewness	Kurtosis
1	0.660	2.721	1.216	1.434	0.560	1.141	3.206
2	0.639	3.755	1.271	1.389	0.581	2.920	13.139
3	0.526	3.684	1.184	1.359	0.611	2.200	9.651
4	0.561	35810.54	288.660	3646.255	7255.685	3.338	16.351
5	0.002	5.068	1.171	1.265	0.867	2.990	15.963
6	0.573	34.604	1.442	4.349	7.470	3.073	12.726
7	0.005	10.812	1.329	1.894	1.902	3.809	20.341

Figures 76 and 77 illustrate the skewness-kurtosis plot of Cullen and Frey for the Landsat extracted Chl-a at all points in Vassova lagoon. Based on these graphs and the AIC and BIC criteria, it occurs that:

a) For Points 1, 2, 3, and 6, the log-normal distribution was found to be the best-fit theoretical distribution;

b) For Points 4, 5 and 7, the gamma distribution was found to be the best-fit theoretical distribution.

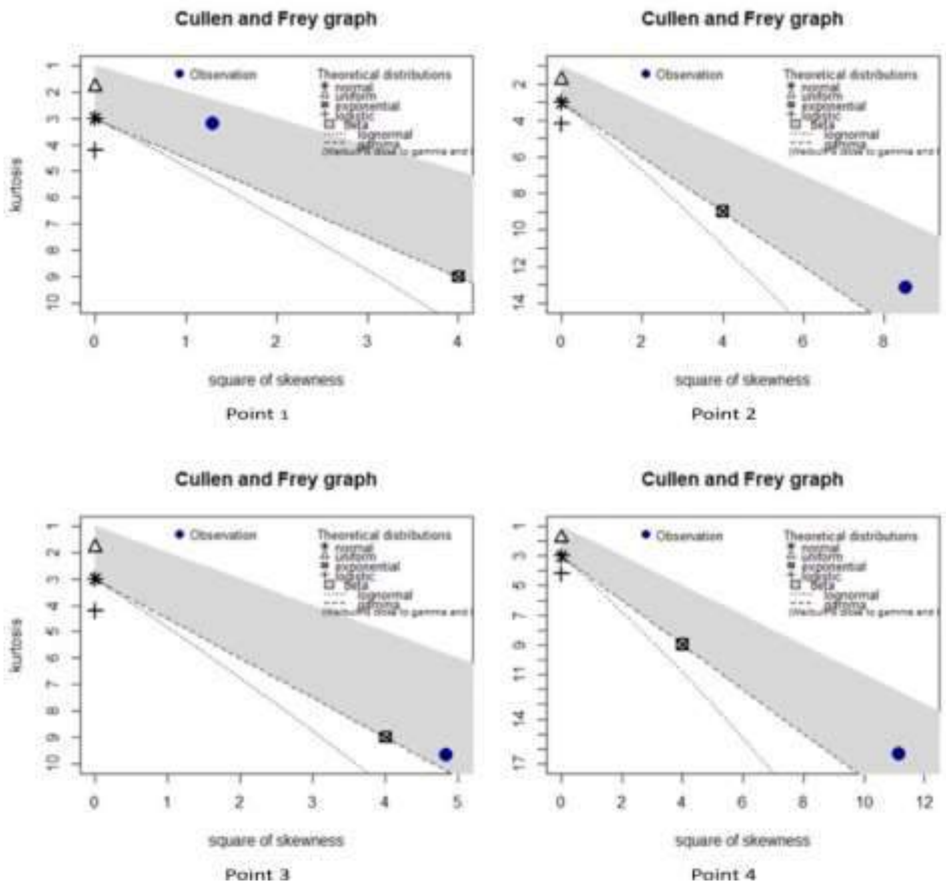

Figure 76. The Cullen and Frey diagrams for the distribution of Chl-a concentration at Points 1 - 4.

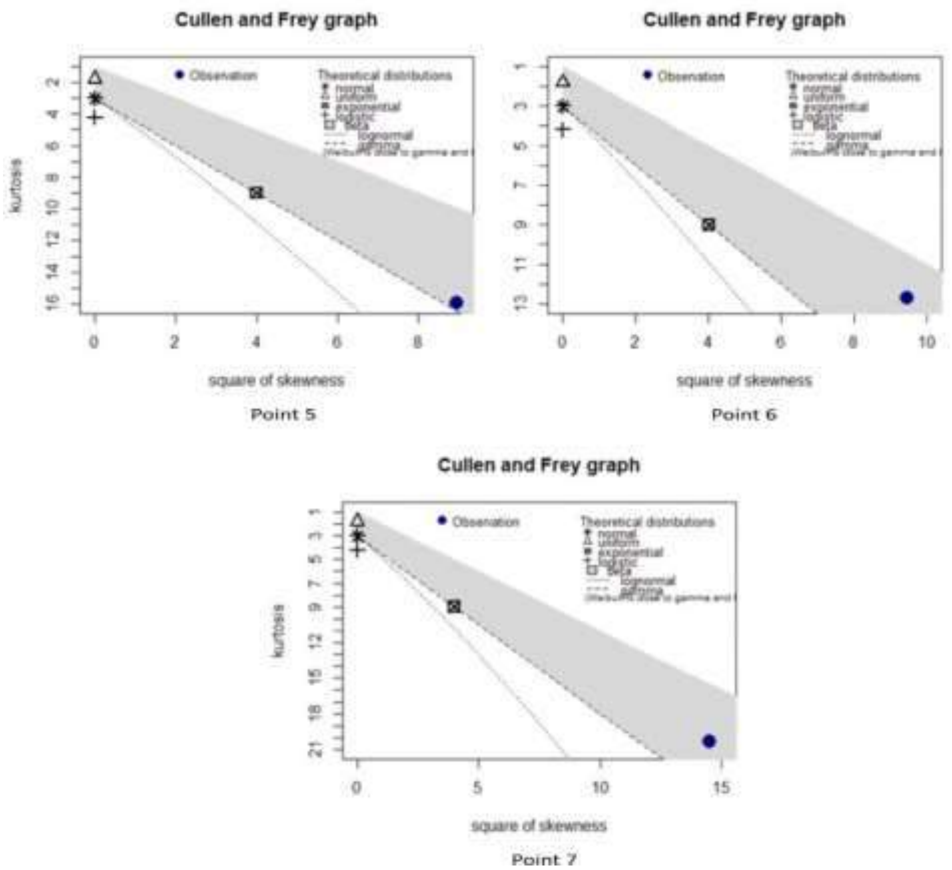

Figure 77. The Cullen and Frey diagrams for the distribution of Chl-a concentration at Points 5 - 7.

Table 9 presents the fitting parameters of the best-fit theoretical probability density function applied on the Chl-a concentration data extracted from Landsat in Vassova lagoon. Mean and standard deviation parameters are given for the normal PDFs, log(mean) and log(sd) parameters for the log-normal distributions and shape and scale for the gamma distributions.

Table 9. Fitting parameters of the best-fit theoretical probability density function.

Points	**1**	**2**	**3**	**4**	**5**	**6**	**7**
Mean							
St Dev							
Log(Mean)	0.296	0.271	0.230			0.764	
Log(St Dev)	0.064	0.058	0.069			0.184	
Shape				0.370	1.467		1.462
Scale							0.215
LogLikelihood	-19.954	-16.154	-20.341	-239.977	-33.887	-65.762	-47.978
AIC	43.908	36.308	44.682	483.954	71.774	135.525	99.956
BIC	46.711	39.110	47.484	486.757	74.576	138.327	102.759

The theoretical probability density functions (PDFs) and the cumulative density functions (CDFs) applied as best-fit on the Chl-a data, together with the relevant Q-to-Q and P-to-P plots are shown in Figures 78 and 79.

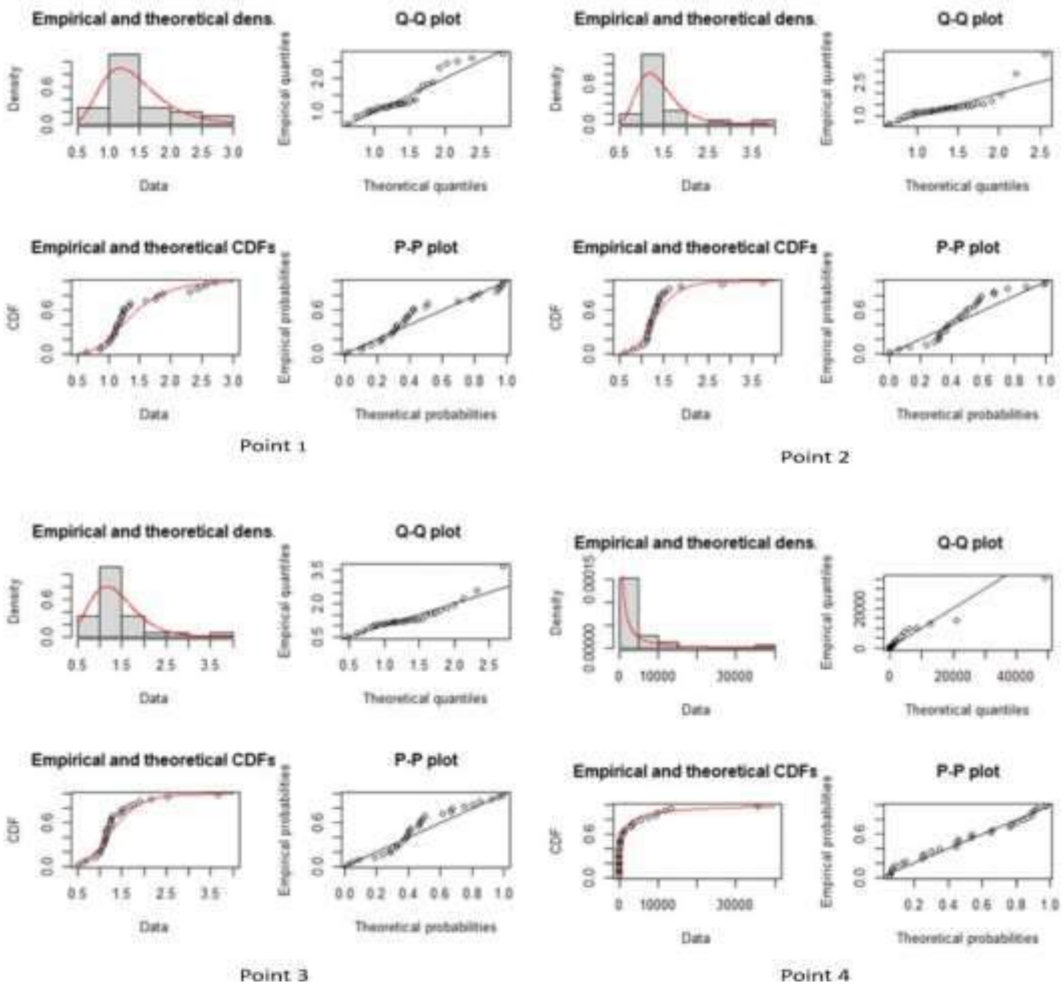

Figure 78. Theoretical probability density functions (PDFs) and the cumulative density functions (CDFs), applied as best-fit on the Chl-a data of points 1 - 4.

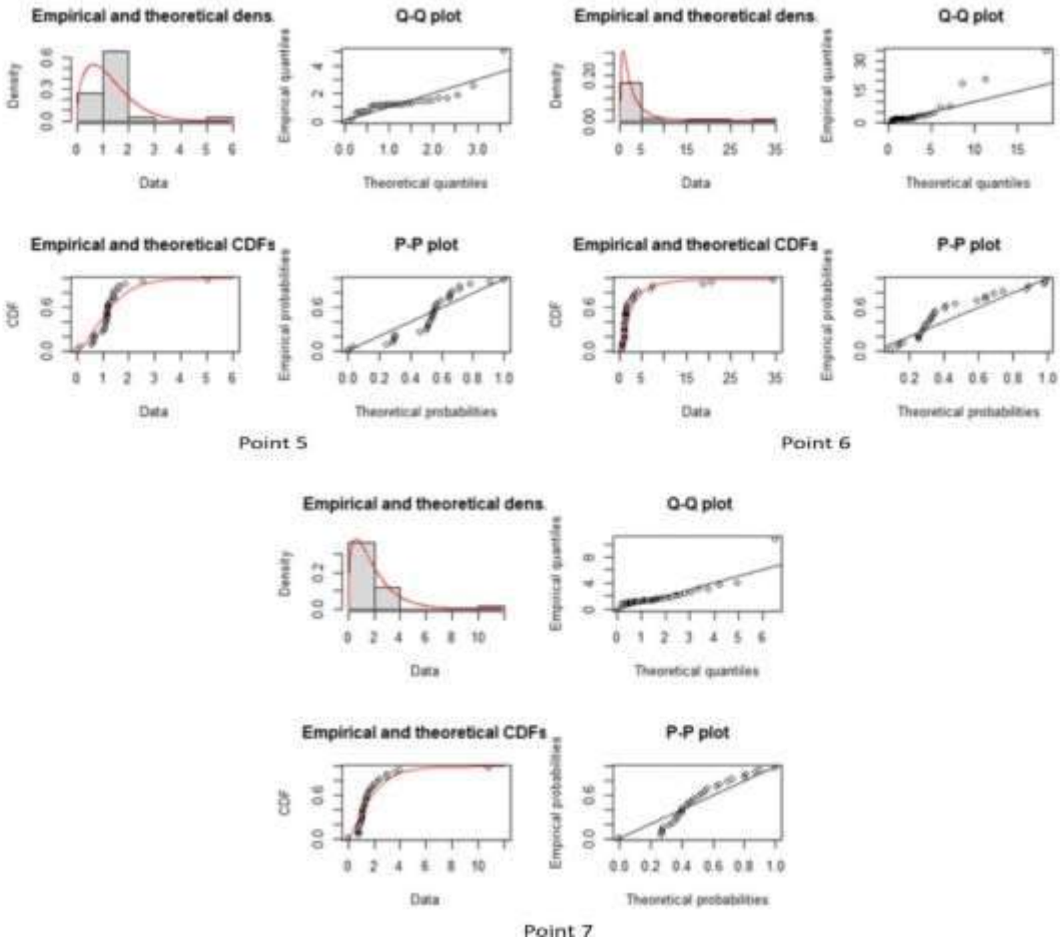

Figure 79. Theoretical probability density functions (PDFs) and the cumulative density functions (CDFs), applied as best-fit on the Chl-a data of points 5 – 7.

Based on the best-fit theoretical CDFs applied on the Chl-a, the probability of exceeding the eutrophication threshold of 2 μg/l was estimated. Probabilities of exceedance for all Vassova lagoon points are summarized in Table 10. Probability is a measure that ranges between 0 and 1, with zero implying that eutrophication is impossible and 1 implying that eutrophication is absolutely certain. Figure 80 illustrates the probability map of exceedance of the eutrophication threshold in Vassova lagoon.

Table 10. Probability of exceedance of the eutrophication threshold in Vassova lagoon.

Points	Probability of Exceedance
1	0.128
2	0.091
3	0.111
4	0.907
5	0.178
6	0.528
7	0.849

Based on the above, points 4, 6 and 7 are more vulnerable to eutrophication effects than the rest of the lagoon. Point 4 is located in the wintering canals, point 6 close to the inlet of the lagoon and point 7 in the north part of the lagoon. For point 6, exceedance probability is approximately 0.5, meaning that during half of a typical year eutrophication may exist. For points 4 and 7 exceedance probability is approximately 0.9 meaning almost the whole typical year eutrophication may exist. Based on the available Landsat images, it seems that the eutrophication prone periods are spring and summer. On the contrary, the rest of the points have limited probability for a eutrophication event.

Figure 80. Probability map of exceedance of the eutrophication threshold in Vassova lagoon.

3.2.1.2 Eratino lagoon

The dataset selected for Chl-a concentration extraction in Eratino lagoon has missing data, hence the eutrophication assessment analysis could not be done.

3.2.1.3 Agiasma lagoon

The points selected for Chl-a concentration extraction for the eutrophication assessment in Agiasma lagoon, are shown in Figure 81. These points cover the typical conditions at all sub-basins of the lagoon and are distributed among various depths.

Figure 81. Points for Chl-a concentration extraction in Agiasma lagoon.

Table 11 presents the statistical measures for Chl-a concentration at all points examined in Agiasma lagoon.

Table 11. Statistical measures per point for Chl-a concentration at Agiasma Lagoon.

Points	Min	Max	Median	Mean	St. deviation	Skewness	Kurtosis
1	0.989	4.580	1.439	1.640	0.699	2.823	12.607
2	1.049	1.679	1.281	1.291	0.163	0.656	2.861
3	0.107	2.818	1.162	1.261	0.438	1.502	8.914
4	0.915	2.339	1.378	1.443	0.328	1.032	4.468
5	0.890	72.135	1.610	3.896	11.923	5.839	37.365
6	1.171	3.826	1.909	1.957	0.558	1.515	6.134
7	0.183	5.098	1.398	1.545	0.769	3.320	17.289
8	0.000	4.552	0.364	0.528	0.758	4.679	27.695

Figures 82 and 83 illustrate the skewness-kurtosis plot of Cullen and Frey for the Landsat extracted Chl-a at all points in Agiasma lagoon. Based on these graphs and the AIC and BIC criteria, it occurs that:

a) For Points 2, 3 and 8, the normal distribution was found to be the best-fit theoretical distribution;
b) For Points 1, 4, 5 and 6, the log-normal distribution was found to be the best-fit theoretical distribution;
c) For Point 7, the gamma distribution was found to be the best-fit theoretical distribution.

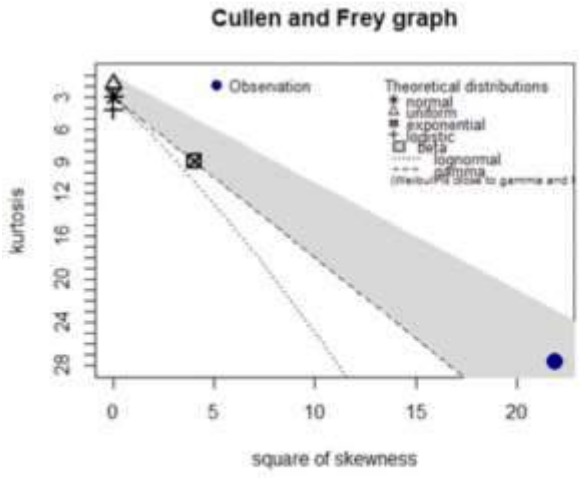

Point 1

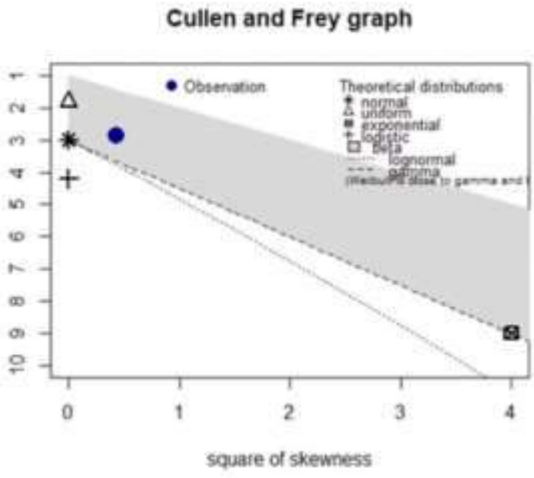

Point 2

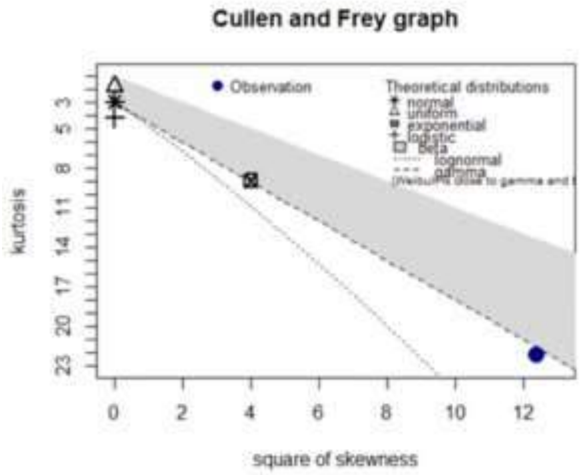

Point 3

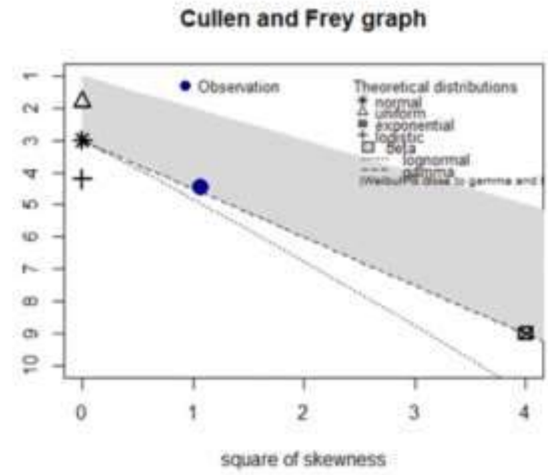

Point 4

Figure 82. The Cullen and Frey diagrams for the distribution of Chl-a concentration at Points 1 - 4.

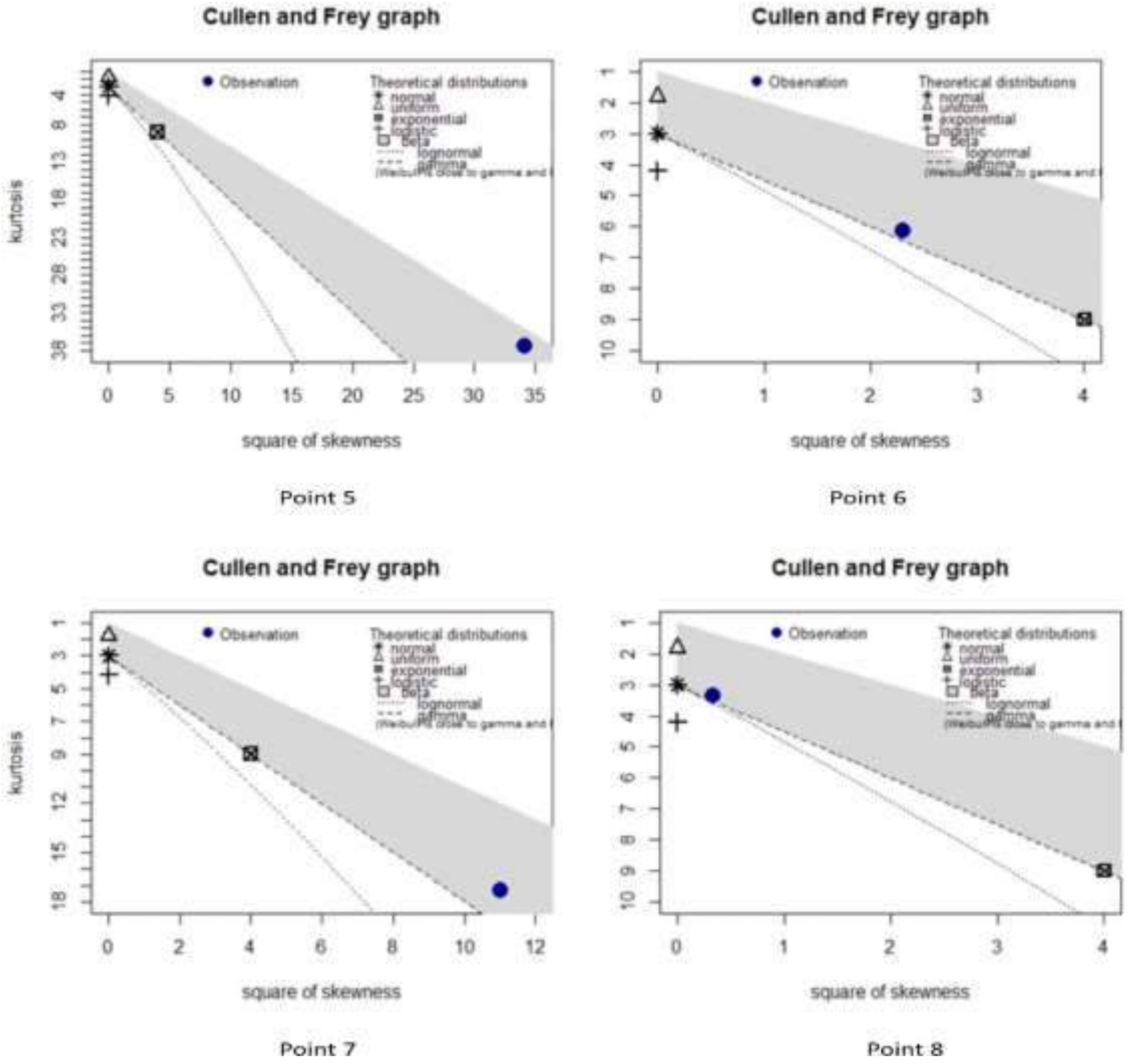

Figure 83. The Cullen and Frey diagrams for the distribution of Chl-a concentration at Points 5 - 8.

Table 12 presents the fitting parameters of the best-fit theoretical probability density function applied on the Chl-a concentration data extracted from Landsat in Agiasma lagoon. Mean and standard deviation parameters are given for the normal PDFs, log(mean) and log(sd) parameters for the log-normal distributions and shape and scale for the gamma distributions.

Table 12. Fitting parameters of the best-fit theoretical probability density function.

Points	**1**	**2**	**3**	**4**	**5**	**6**	**7**	**8**
Mean		1.291	1.261					1.272
St Dev		0.161	0.431					0.248
Log(Mean)	0.434			0.343	0.631	0.637		
Log(St Dev)	0.054			0.213	0.759	0.255		

Shape							5.506	
Scale							3.563	
LogLikelihood	-24.941	14.232	-20.264	-7.717	-62.136	-24.169	-32.825	-0.957
AIC	53.883	-24.465	44.529	19.434	128.272	52.339	69.650	5.914
BIC	56.994	-21.354	47.639	22.545	131.382	55.450	72.761	9.025

The theoretical probability density functions (PDFs) and the cumulative density functions (CDFs) applied as best-fit on the Chl-a data, together with the relevant Q-to-Q and P-to-P plots are shown in Figures 84 and 85.

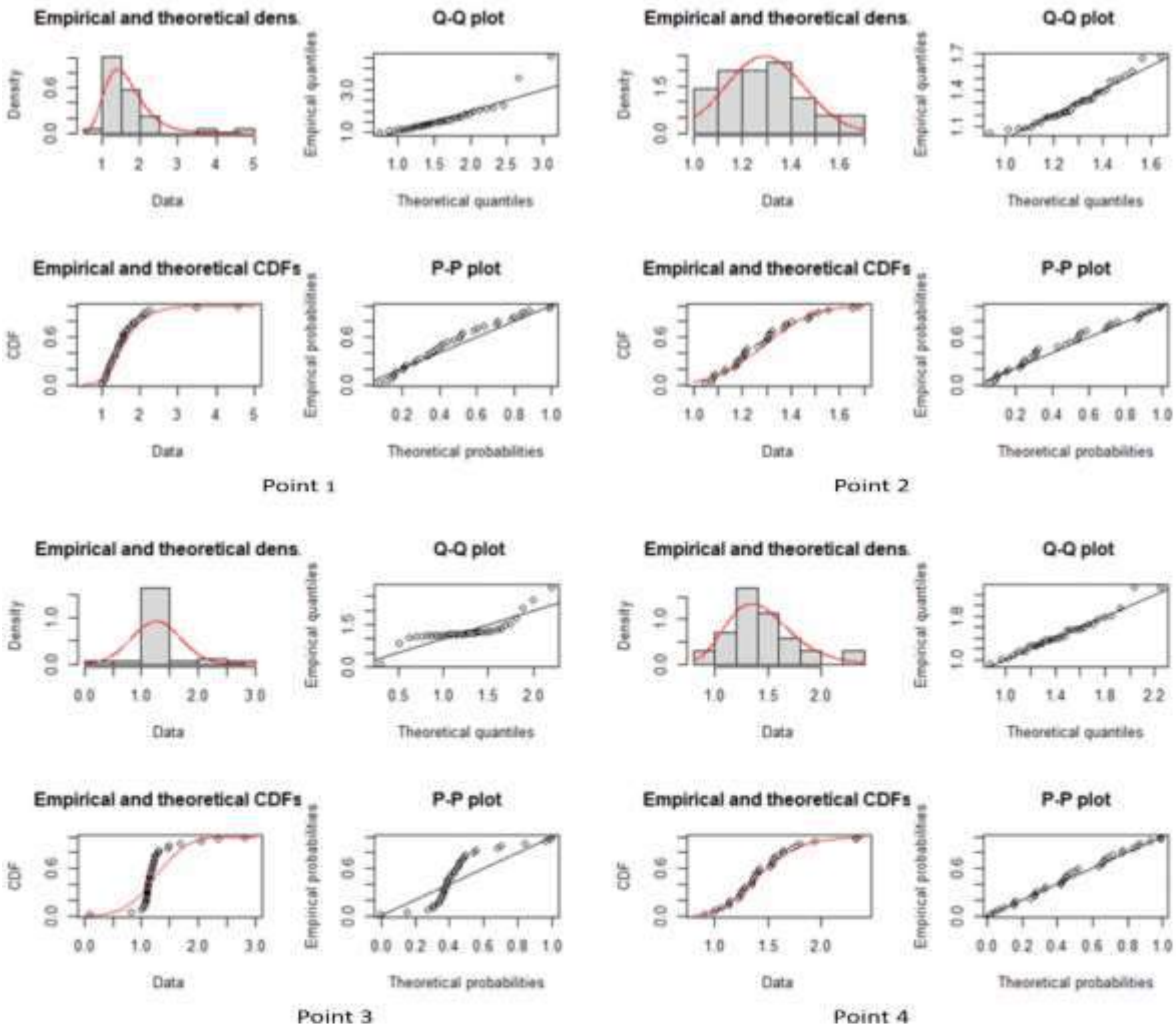

Figure 84. Theoretical probability density functions (PDFs) and the cumulative density functions (CDFs), applied as best-fit on the Chl-a data of points 1 – 4.

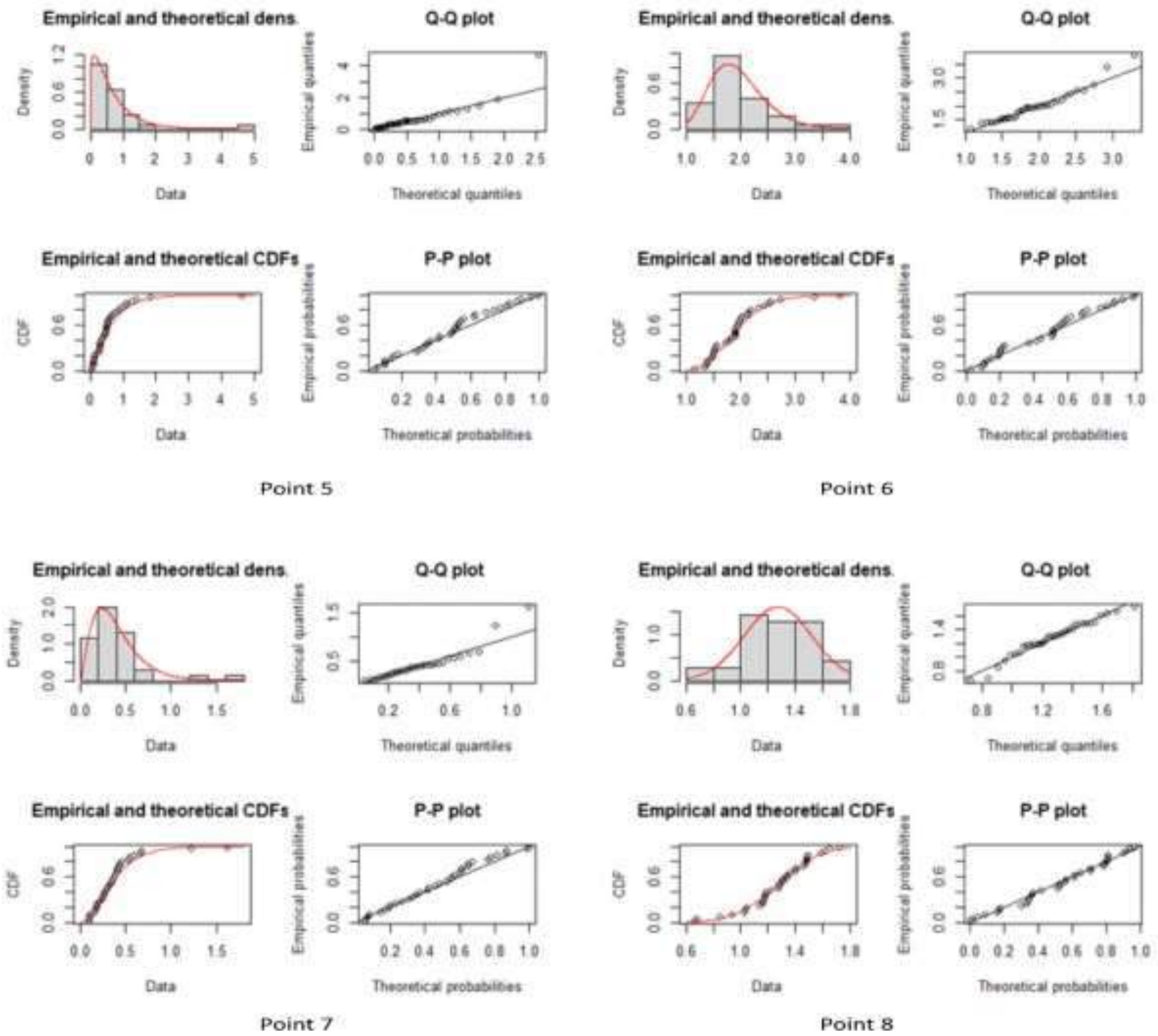

Figure 85. Theoretical probability density functions (PDFs) and the cumulative density functions (CDFs), applied as best-fit on the Chl-a data of points 5 – 8.

Based on the best-fit theoretical CDFs applied on the Chl-a, the probability of exceeding the eutrophication threshold of 2 μg/l was estimated. Probabilities of exceedance for all Agiasma lagoon points are summarized in Table 13. Probability is a measure that ranges between 0 and 1, with zero implying that eutrophication is impossible and 1 implying that eutrophication is absolutely certain. Figure 86 illustrates the probability map of exceedance of the eutrophication threshold in Agiasma lagoon.

Table 13. Probability of exceedance of the eutrophication threshold in Agiasma lagoon.

Points	Probability of Exceedance
1	0.209
2	5.442e-06
3	0.043

4	0.051
5	0.467
6	0.413
7	0.220
8	0.001

Based on the above, points 1, 5 and 6 are more vulnerable to eutrophication effects than the rest of the lagoon. These points are located at the vicinity of the northern inlet of the lagoon and its central basin. Exceedance probability is approx. 0.5, meaning that during half of a typical year eutrophication may exist. Based on the available Landsat images, it seems that the eutrophication prone periods are spring and summer. On the contrary, points located near the southern inlet have limited probability for a eutrophication event.

Figure 86. Probability map of exceedance of the eutrophication threshold in Agiasma lagoon.

3.2.1.4 Porto Lagos lagoon

The points selected for Chl-a concentration extraction for the eutrophication assessment in Porto Lagos lagoon, are shown in Figure 87. These points cover the typical conditions at all sub-basins of the lagoon and are distributed among various depths.

Figure 87. Points for Chl-a concentration extraction in Porto Lagos lagoon.

Table 14 presents the statistical measures for Chl-a concentration at all points examined in Porto Lagos lagoon.

Table 14. Statistical measures per point for Chl-a concentration at Porto Lagos lagoon.

Points	Min	Max	Median	Mean	St. deviation	Skewness	Kurtosis
1	1.036	5.086	1.731	1.939	0.782	2.273	9.929
2	0.080	2.708	1.009	1.042	0.566	0.832	3.793
3	1.108	9.246	4.734	4.748	2.103	0.063	2.209
4	-0.490	1.061	0.294	0.341	0.306	0.176	4.510
5	-0.228	1.245	0.330	0.403	0.314	0.618	3.364
6	1.084	4.403	1.600	1.835	0.698	2.064	7.838
7	0.926	3.802	1.322	1.629	0.680	1.860	5.926
8	1.006	22.340	1.417	2.270	3.554	5.610	35.431
9	0.959	3.591	1.368	1.517	0.506	2.154	10.202
10	1.042	5.002	1.624	1.729	0.724	2.955	14.986
11	0.899	75.929	1.505	3.708	12.578	5.899	37.859
12	0.858	3.974	1.512	1.592	0.508	3.149	17.105
13	0.024	707.430	2.771	64.424	174.313	3.213	12.408

Figures 88, 89 and 90 illustrate the skewness-kurtosis plot of Cullen and Frey for the Landsat extracted Chl-a at all points in Porto Lagos lagoon. Based on these graphs and the AIC and BIC criteria, it occurs that:

a) For Point 3, the gamma distribution was found to be the best-fit theoretical distribution;
b) For all the other points (1-2 and 4-13), the log-normal distribution was found to be the best-fit theoretical distribution.

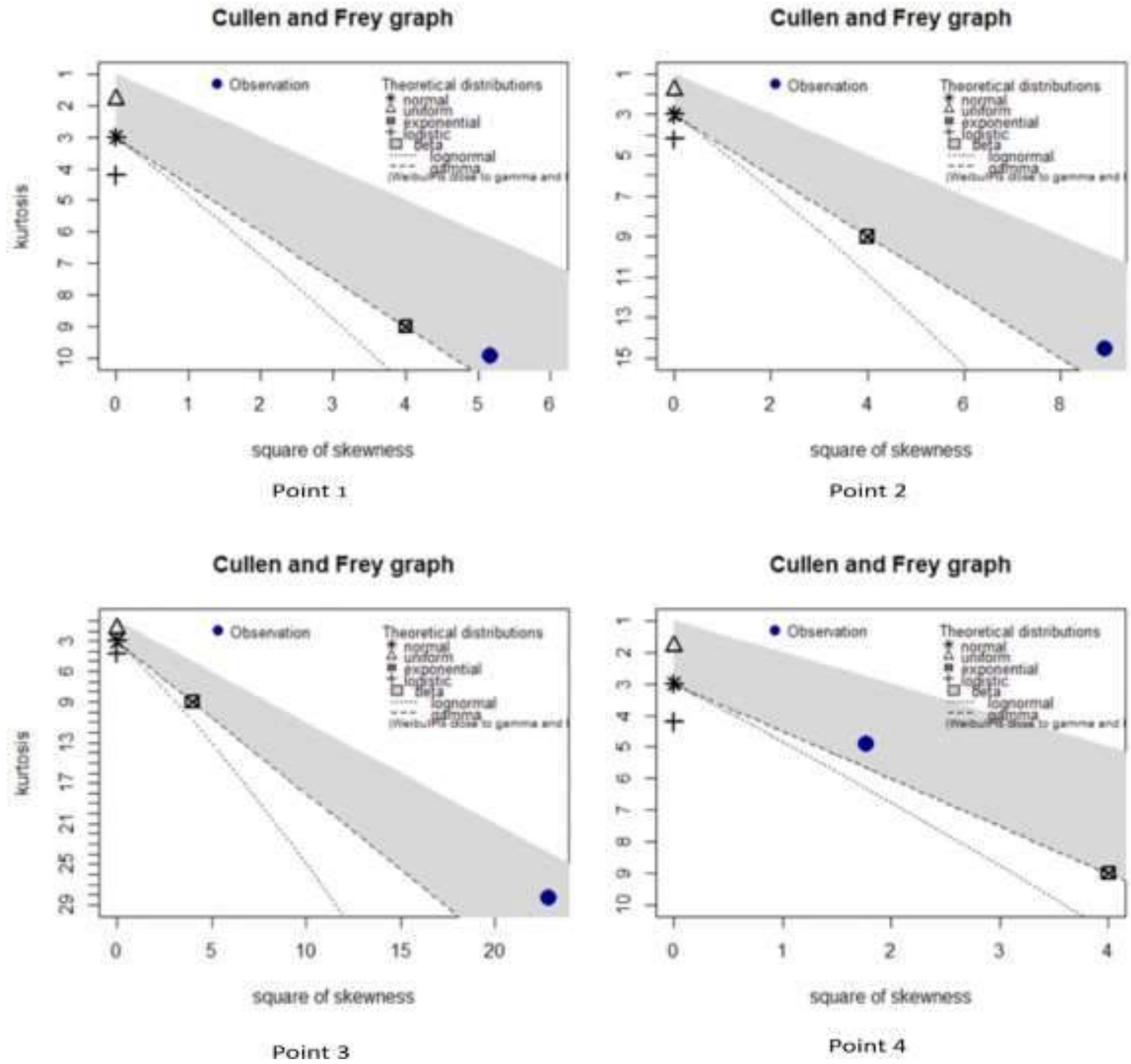

Figure 88. The Cullen and Frey diagrams for the distribution of Chl-a concentration at Points 1 - 4.

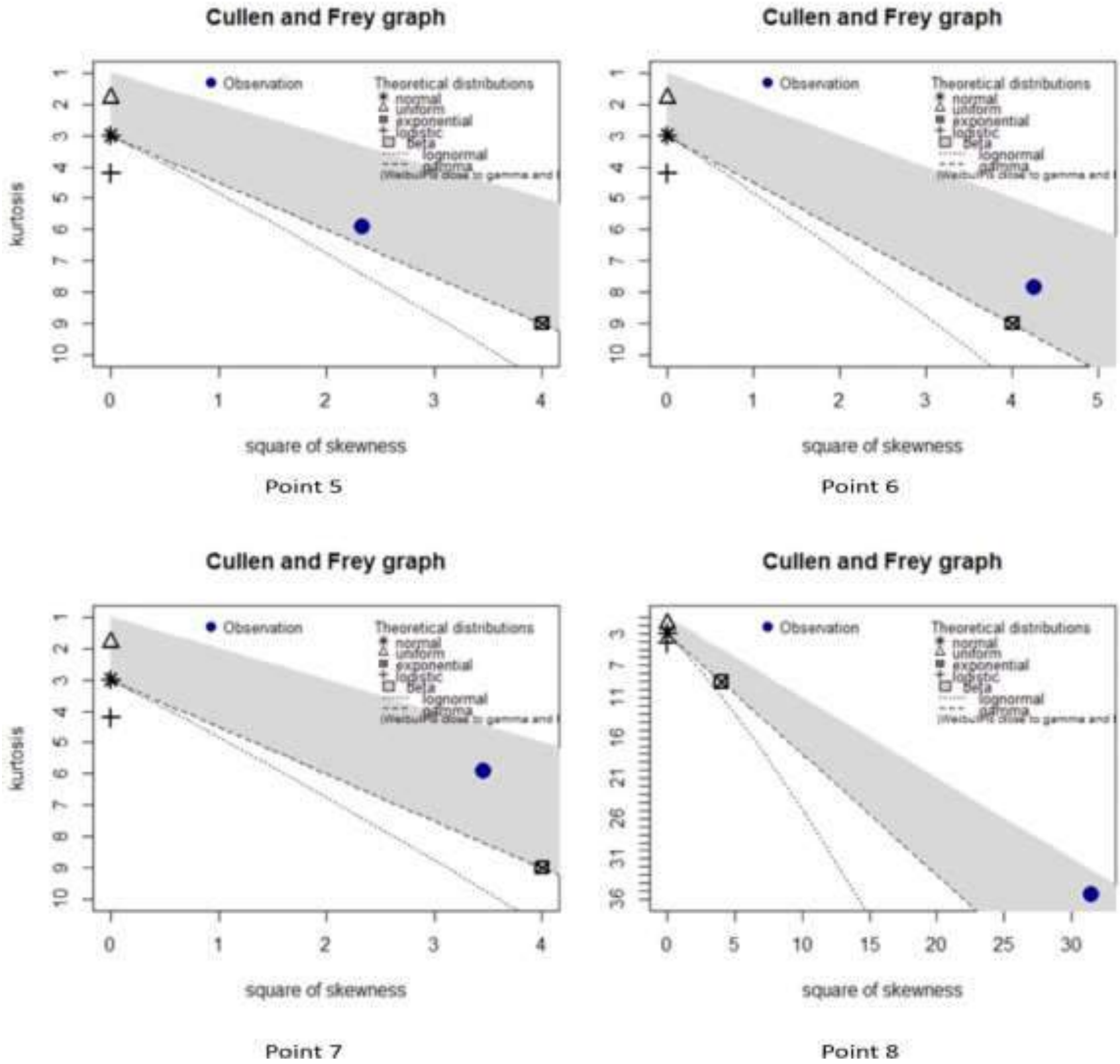

Figure 89. The Cullen and Frey diagrams for the distribution of Chl-a concentration at Points 5 - 8.

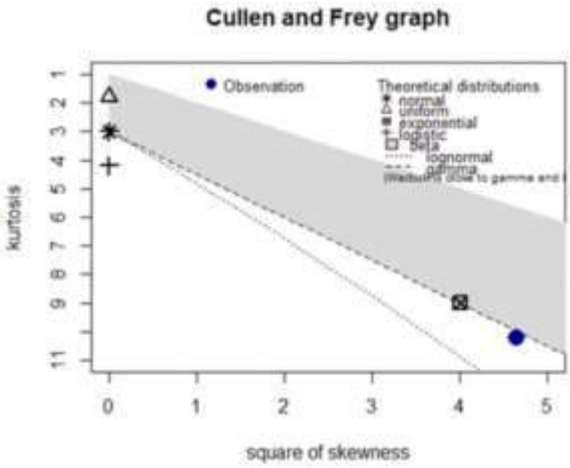

Point 9

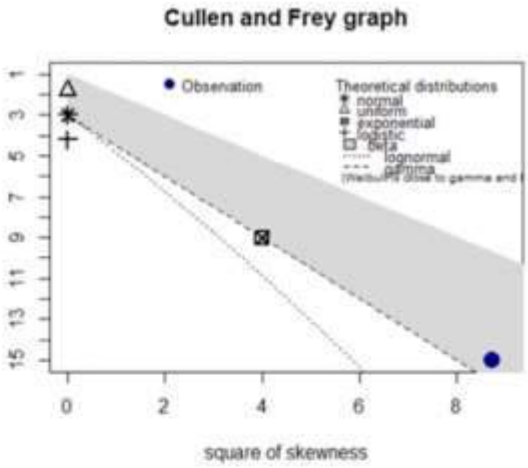

Point 10

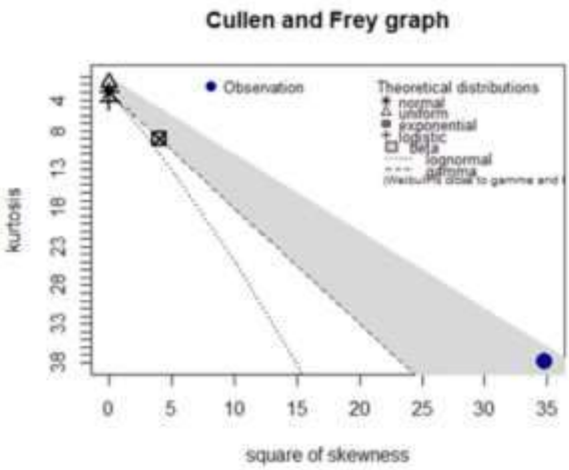

Point 11

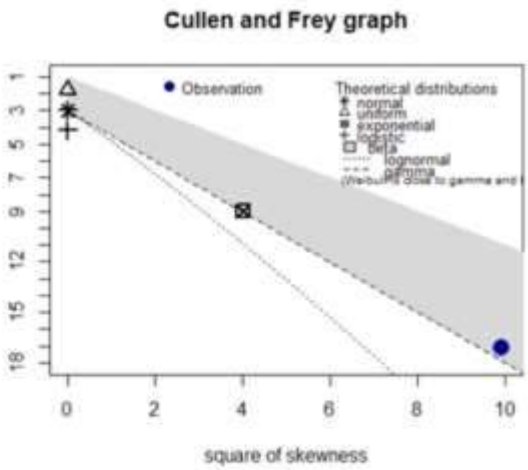

Point 12

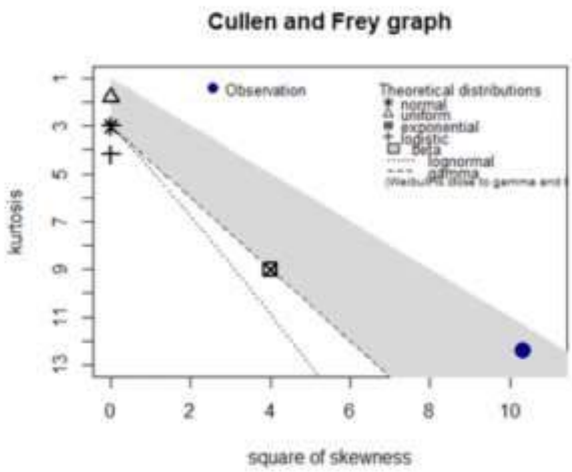

Point 13

Figure 90. The Cullen and Frey diagrams for the distribution of Chl-a concentration at Points 9 - 13.

Table 15 presents the fitting parameters of the best-fit theoretical probability density function applied on the Chl-a concentration data extracted from Landsat in Porto Lagos lagoon. Mean and standard deviation parameters are given for the normal PDFs, log(mean) and log(sd) parameters for the log-normal distributions and shape and scale for the gamma distributions.

Table 15. Fitting parameters of the best-fit theoretical probability density function.

Points	**1**	**2**	**3**	**4**	**5**	**6**	**7**
Mean							
St Dev							
Log(Mean)	0.603	1.042		0.341	0.403	0.553	0.424
Log(St Dev)	0.0554	0.094		0.051	0.052	0.052	0.057
Shape			2.928				
Scale			0.862				
LogLikelihood	-31.682	-65.743	-69.323	-19.684	-22.773	-27.962	-26.251
AIC	67.364	135.487	142.646	43.369	49.545	59.925	56.501
BIC	70.474	138.598	145.757	46.480	52.656	63.035	59.612
Points	**8**	**9**	**10**	**11**	**12**	**13**	
Mean							
St Dev							
Log(Mean)	0.534	0.373	0.488	0.531	0.429	1.465	
Log(St Dev)	0.092	0.047	0.054	0.119	0.043	0.373	
Shape							
Scale							
LogLikelihood	-47.296	-18.402	-27.064	-55.879	-16.570	-128.607	
AIC	98.592	40.804	58.128	115.757	37.139	261.213	
BIC	101.703	43.914	61.234	118.868	40.250	264.324	

The theoretical probability density functions (PDFs) and the cumulative density functions (CDFs) applied as best-fit on the Chl-a data, together with the relevant Q-to-Q and P-to-P plots are shown in Figures 91, 92 and 93.

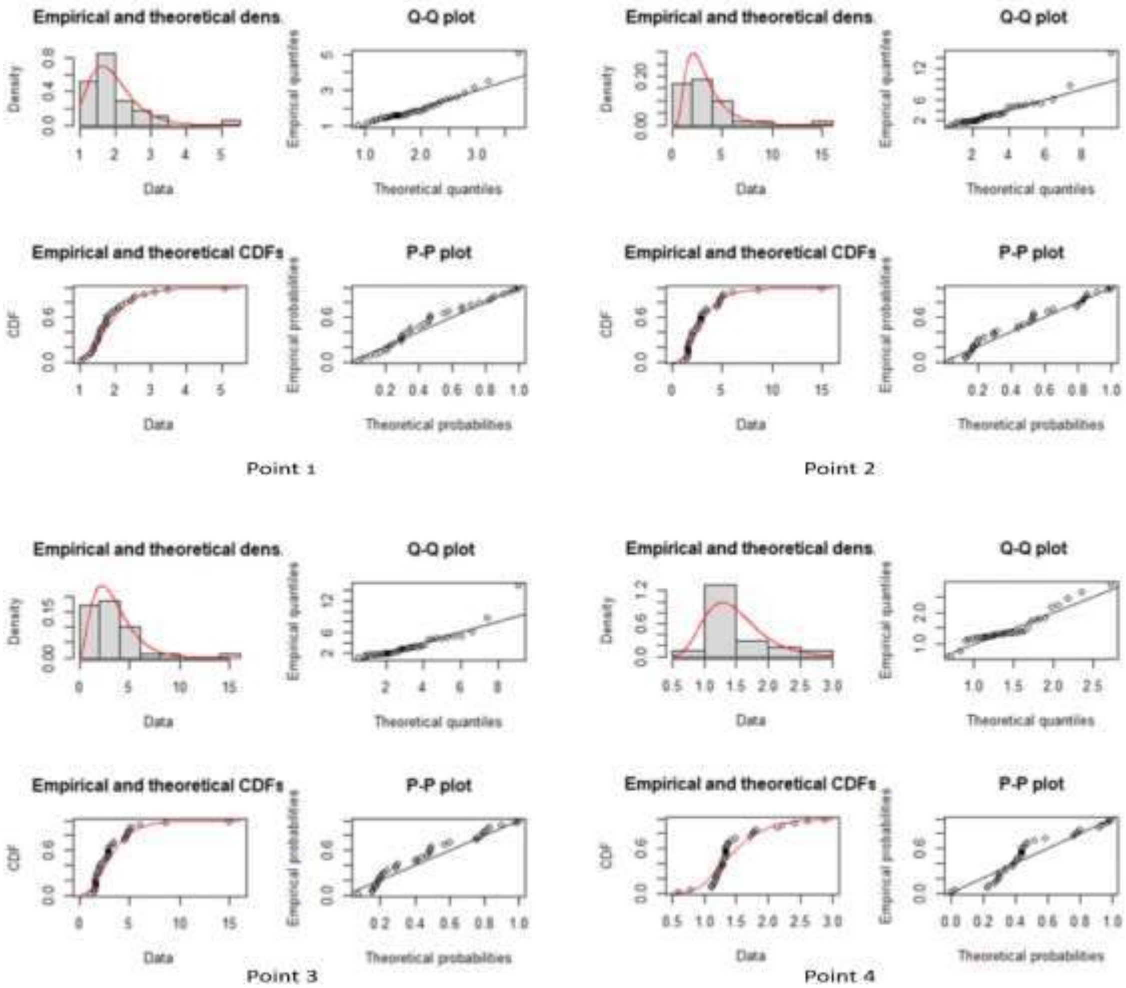

Figure 91. Theoretical probability density functions (PDFs) and the cumulative density functions (CDFs), applied as best-fit on the Chl-a data of points 1 – 4.

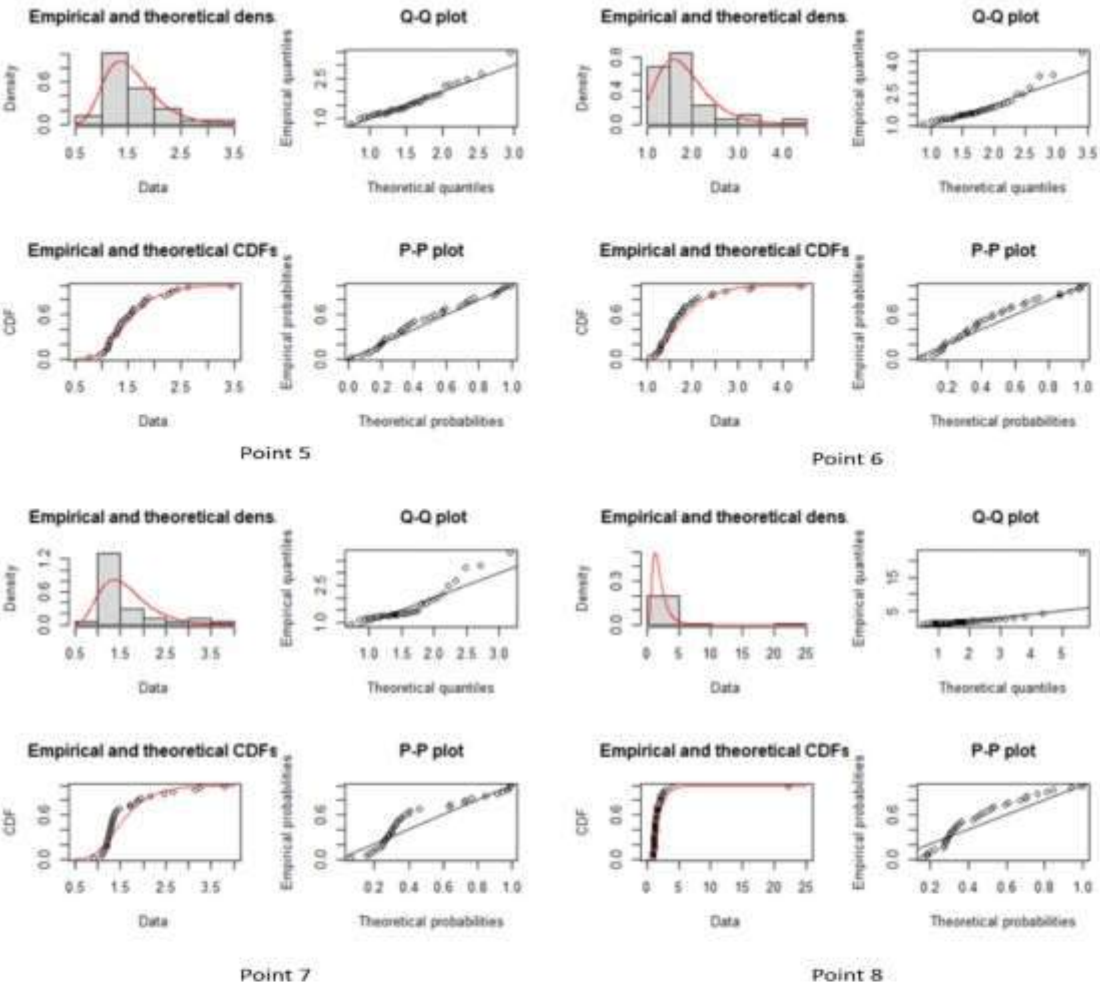

Figure 92. Theoretical probability density functions (PDFs) and the cumulative density functions (CDFs), applied as best-fit on the Chl-a data of points 5 – 8.

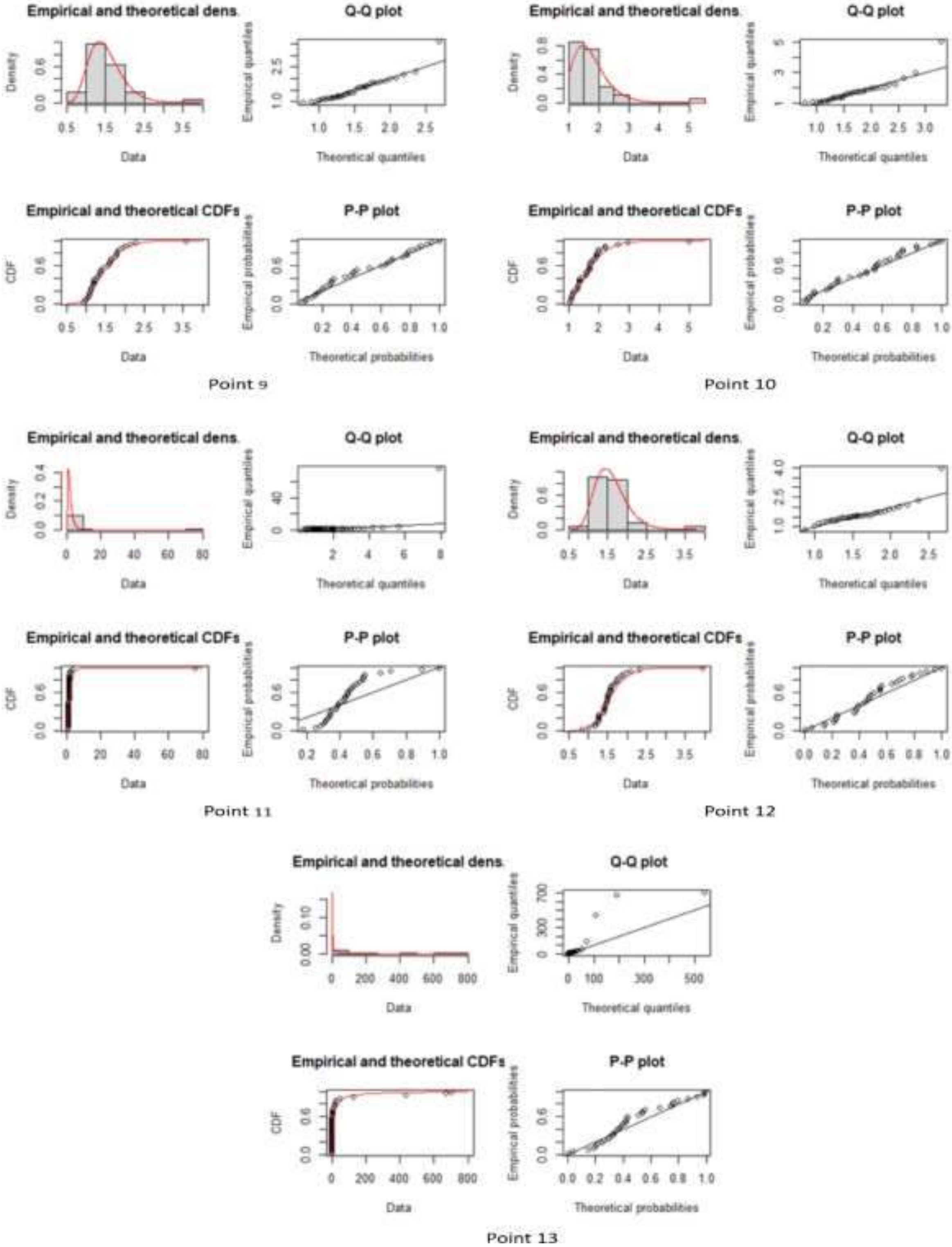

Figure 93. Theoretical probability density functions (PDFs) and the cumulative density functions (CDFs), applied as best-fit on the Chl-a data of points 9 – 13.

Based on the best-fit theoretical CDFs applied on the Chl-a, the probability of exceeding the eutrophication threshold of 2 μg/l was estimated. Probabilities of exceedance for all Porto Lagos lagoon points are summarized in Table 16. Probability is a measure that ranges between 0 and 1, with zero implying that eutrophication is impossible and 1 implying that eutrophication is absolutely certain. Figure 94 illustrates the probability map of exceedance of the eutrophication threshold in Porto Lagos lagoon.

Table 16. Probability of exceedance of the eutrophication threshold in Porto Lagos lagoon.

Points	Probability of Exceedance
1	0.391
2	0.734
3	0.989
4	0.122
5	0.175
6	0.326
7	0.211
8	0.386
9	0.128
10	0.262
11	0.409
12	0.148
13	0.637

Based on the above, points 2, 3 and 13 are more vulnerable to eutrophication effects than the rest of the lagoon. Points 2 and 3 are located in the small canals inside the lagoon connecting the two main sub-basins of the lagoon and 13 close to the inlet of the lagoon. Exceedance probability ranges from 0.6 to almost 1, eutrophication may exist for almost the whole typical year. Based on the available Landsat images, it seems that the eutrophication prone periods are spring and summer. The rest of the points have limited probability for a eutrophication event.

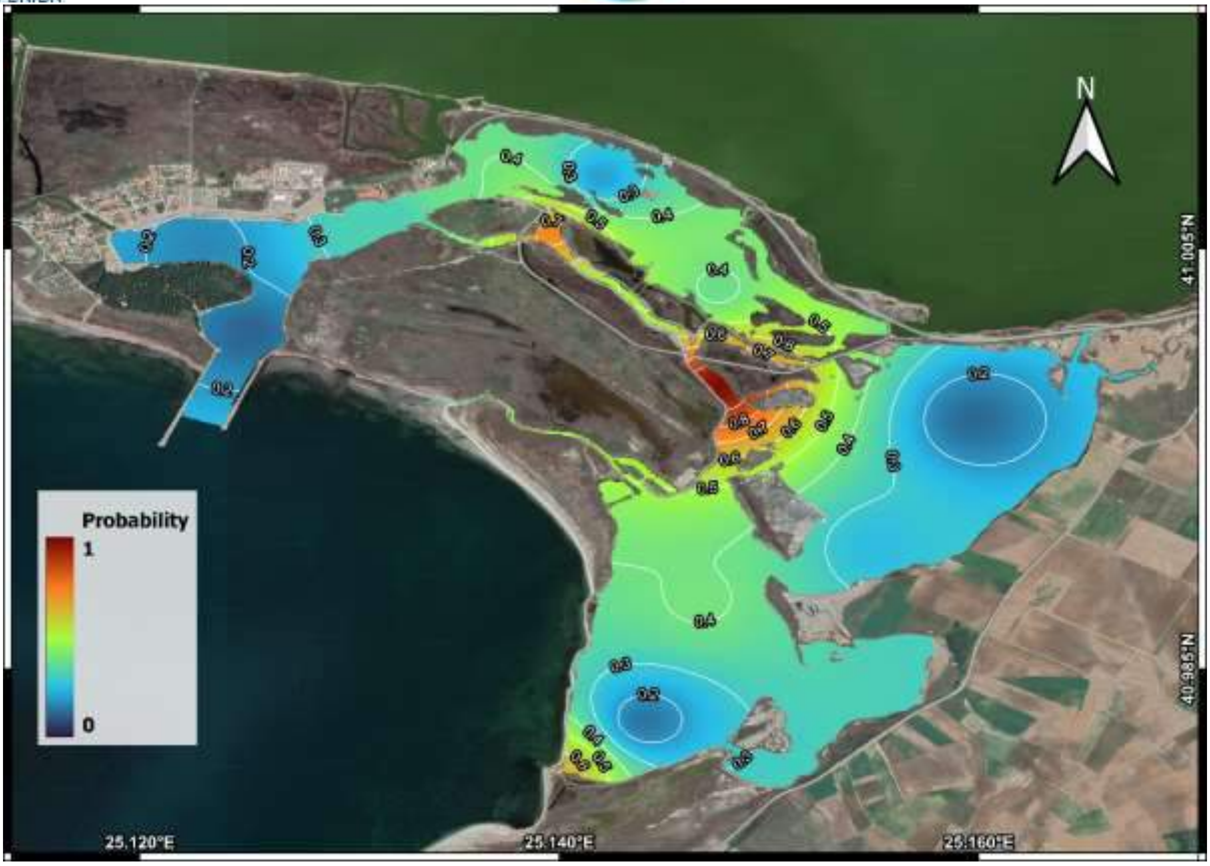

Figure 94. Probability map of exceedance of the eutrophication threshold in Porto Lagos lagoon.

3.2.1.5 Xirolimni

The points selected for Chl-a concentration extraction for the eutrophication assessment in Xirolimni lagoon, are shown in Figure 95. These points cover the typical conditions of the lagoon and are distributed among various depths.

Figure 95. Points for Chl-a concentration extraction in Xirolimni lagoon.

Table 17 presents the statistical measures for Chl-a concentration at all points examined in Xirolimni lagoon.

Table 17. Statistical measures per point for Chl-a concentration at Xirolimni Lagoon.

Points	Min	Max	Median	Mean	St. deviation	Skewness	Kurtosis
1	0.668	11.183	1.415	1.993	1.842	4.680	22.054
2	0.516	3.079	1.290	1.313	0.448	1.706	9.299
3	0.002	1.743	0.394	0.502	0.474	1.099	3.892
4	0.634	3.448	1.311	1464	0.626	1.430	5.056
5	0.560	17.902	1.315	1.793	2.820	5.806	37.113
6	0.402	5.104	1.345	1.587	0.944	2.242	8.888
7	0.448	1.800	1.214	1.216	0.270	-0.596	4.750

Figures 96 and 97 illustrate the skewness-kurtosis plot of Cullen and Frey for the Landsat extracted Chl-a at all points in Xirolimni lagoon. Based on these graphs and the AIC and BIC criteria, it occurs that:

a) For Points 1, 4, 5 and 6, the log-normal distribution was found to be the best-fit theoretical distribution;
b) For Points 2,3 and 7, the gamma distribution was found to be the best-fit theoretical distribution.

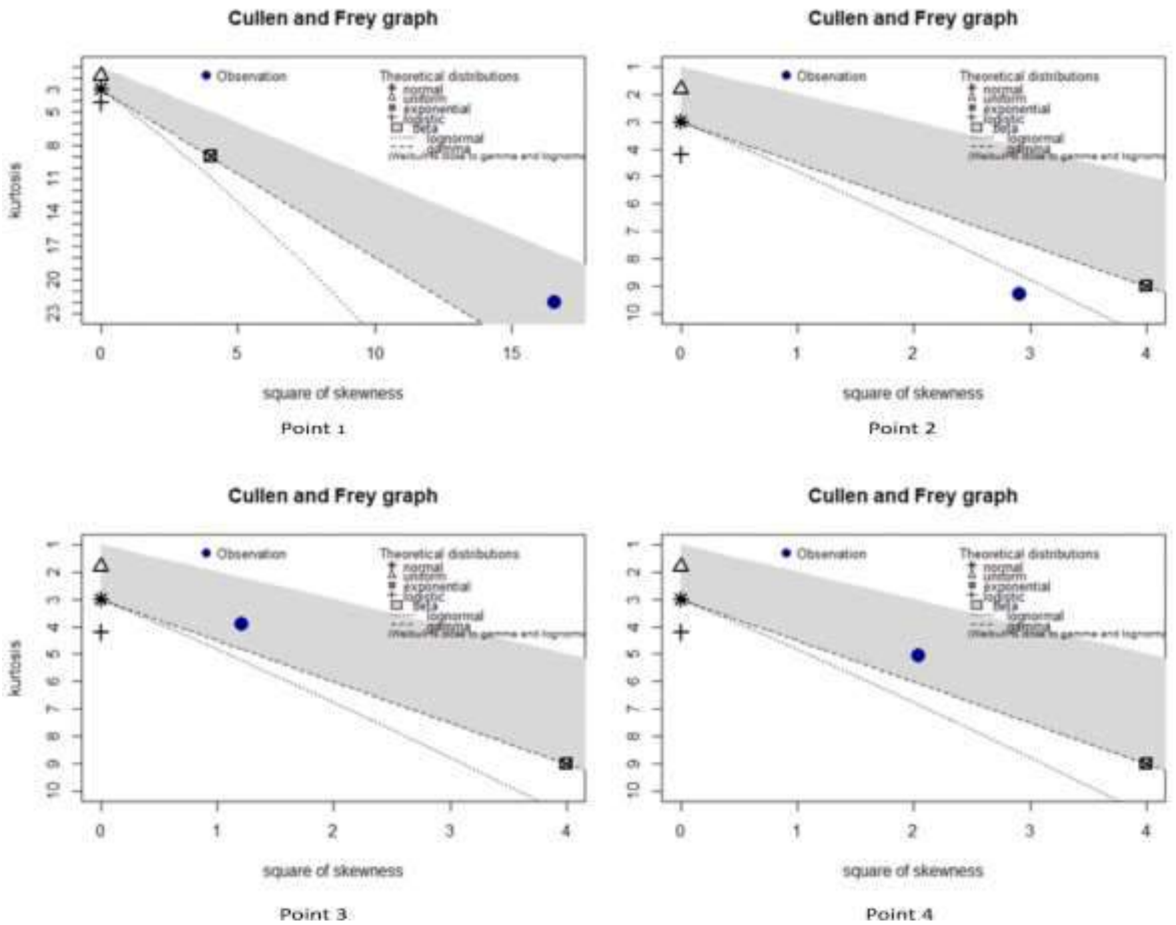

Figure 96. The Cullen and Frey diagrams for the distribution of Chl-a concentration at Points 1 - 4.

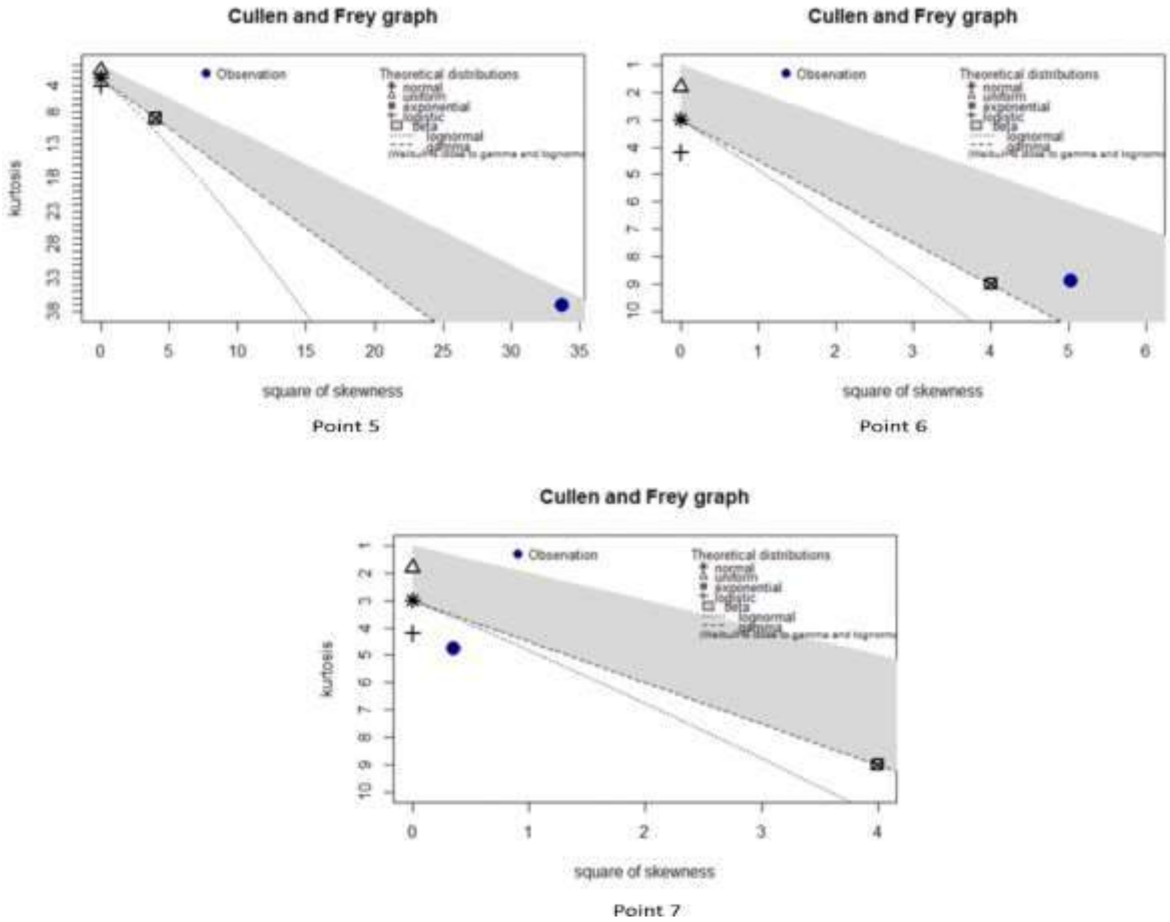

Figure 97. The Cullen and Frey diagrams for the distribution of Chl-a concentration at Points 5 - 7.

Table 18 presents the fitting parameters of the best-fit theoretical probability density function applied on the Chl-a concentration data extracted from Landsat in Xirolimni lagoon. Mean and standard deviation parameters are given for the normal PDFs, log(mean) and log(sd) parameters for the log-normal distributions and shape and scale for the gamma distributions.

Table 18. Fitting parameters of the best-fit theoretical probability density function.

Points	1	2	3	4	5	6	7
Mean							
St Dev							
Log(Mean)	0.498			0.305	0.321	0.332	
Log(St Dev)	0.090			0.064	0.086	0.084	
Shape		9.792	0.878				5.247
Scale		7.456	0.474				1.317
LogLikelihood	-45.173	-18.051	-10.414	-26.678	-37.398	-36.608	-2.999
AIC	94.346	40.102	24.828	57.356	78.795	77.216	10.000

BIC	97.456	43.212	27.939	60.466	81.906	80.326	13.108

The theoretical probability density functions (PDFs) and the cumulative density functions (CDFs) applied as best-fit on the Chl-a data, together with the relevant Q-to-Q and P-to-P plots are shown in Figures 98 and 99.

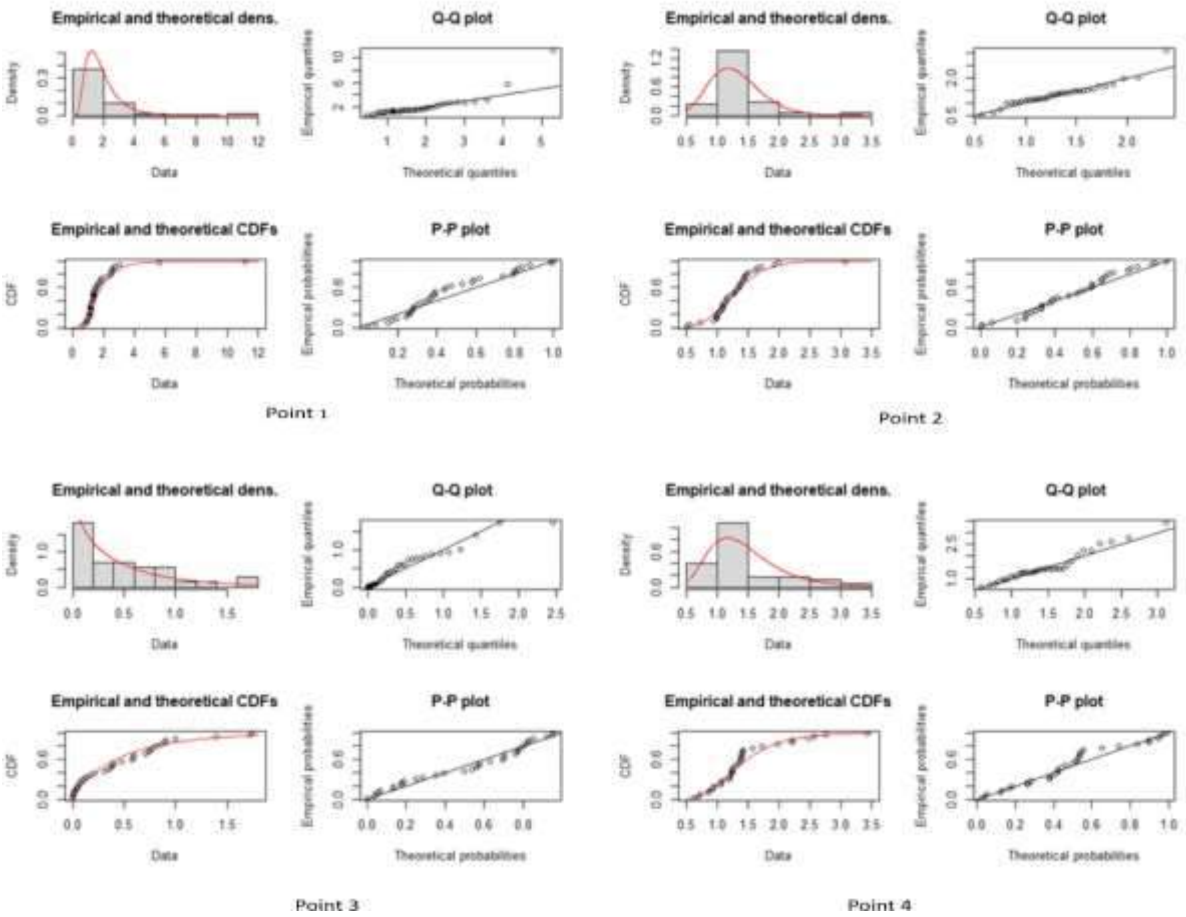

Figure 98. Theoretical probability density functions (PDFs) and the cumulative density functions (CDFs), applied as best-fit on the Chl-a data of points 1 – 4.

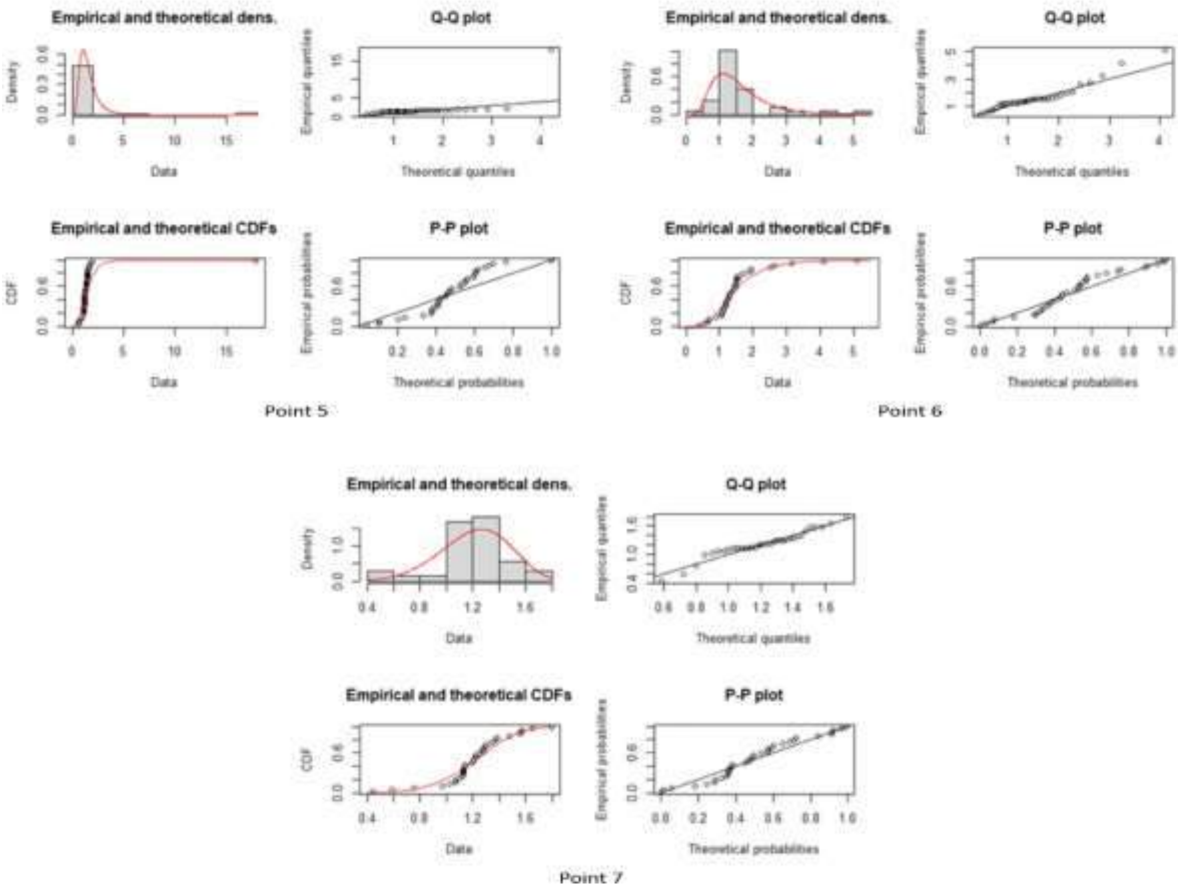

Figure 99. Theoretical probability density functions (PDFs) and the cumulative density functions (CDFs), applied as best-fit on the Chl-a data of points 5 – 7.

Based on the best-fit theoretical CDFs applied on the Chl-a, the probability of exceeding the eutrophication threshold of 2 μg/l was estimated. Probabilities of exceedance for all Xirolimni lagoon points are summarized in Table 19. Probability is a measure that ranges between 0 and 1, with zero implying that eutrophication is impossible and 1 implying that eutrophication is absolutely certain. Figure 100 illustrates the probability map of exceedance of the eutrophication threshold in Xirolimni lagoon.

Table 19. Probability of exceedance of the eutrophication threshold in Xirolimni lagoon.

Points	**Probability of Exceedance**
1	0.358
2	0.073
3	0.030
4	0.155
5	0.233
6	0.232
7	0.000

Based on the above, exceedance probability for all points is below 0.5, meaning they have limited probability for a eutrophication event.

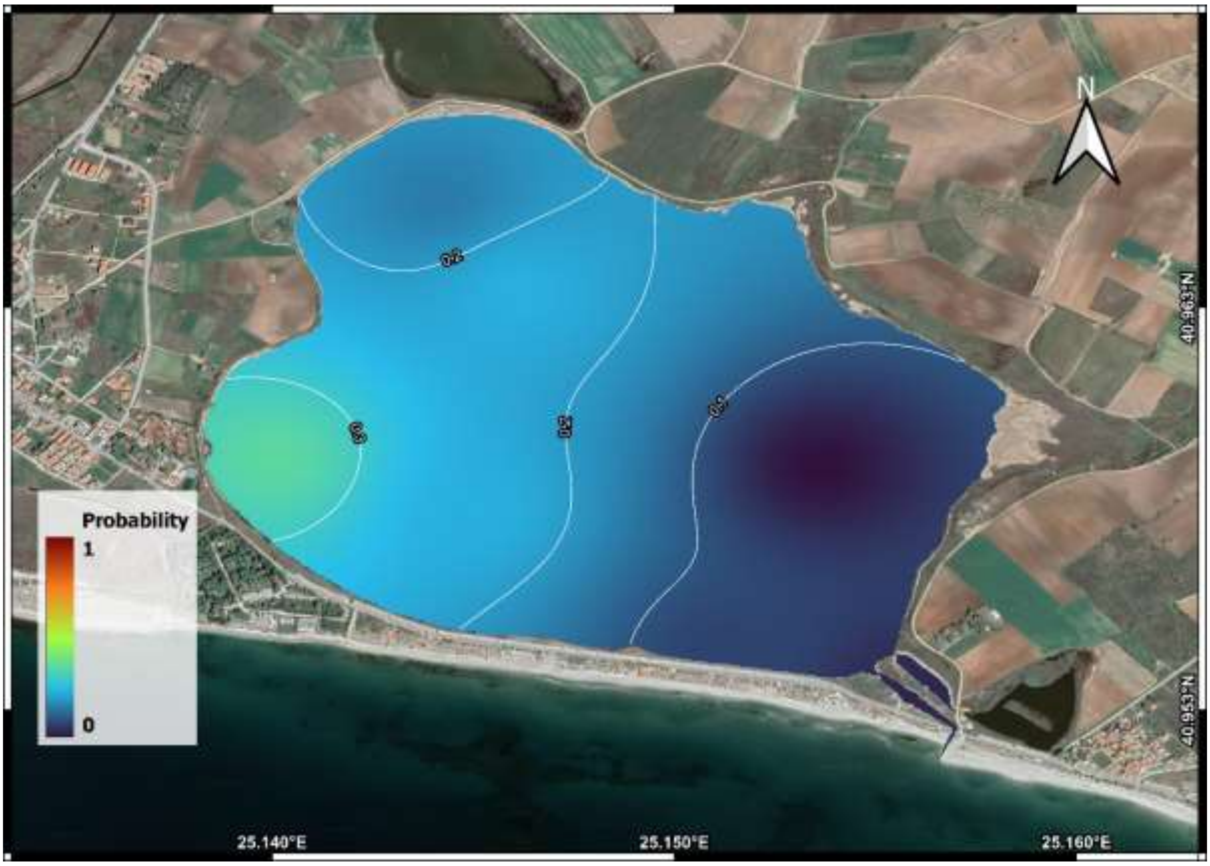

Figure 100. Probability map of exceedance of the eutrophication threshold in Xirolimni lagoon.

3.2.1.6 *Ptelea*

The points selected for Chl-a concentration extraction for the eutrophication assessment in Ptelea lagoon, are shown in Figure 101. These points cover the typical conditions of the lagoon and are distributed among various depths.

Figure 101. Points for Chl-a concentration extraction in Ptelea lagoon.

Table 20 presents the statistical measures for Chl-a concentration at all points examined in Ptelea lagoon.

Table 20. Statistical measures per point for Chl-a concentration at Ptelea Lagoon.

Points	Min	Max	Median	Mean	St. deviation	Skewness	Kurtosis
1	0.009	9.097	1.195	1.380	1.462	4.585	27.131
2	0.043	1238.171	1.192	55.386	231.934	4.611	24.820
4	0.008	124.978	1.550	5.936	21.347	5.456	33.732
5	0.011	19.165	1.206	2.067	3.784	3.991	18.613
6	0.003	2.557	1.257	1.218	0.552	0.126	3.440

Figure 102 illustrates the skewness-kurtosis plot of Cullen and Frey for the Landsat extracted Chl-a at all points in Ptelea lagoon. Based on these graphs and the AIC and BIC criteria, it occurs that:

a) For Point 6, the normal distribution was found to be the best-fit theoretical distribution;
b) For Points 2, 4, and 5, the log-normal distribution was found to be the best-fit theoretical distribution;
c) For Point 1, the gamma distribution was found to be the best-fit theoretical distribution.

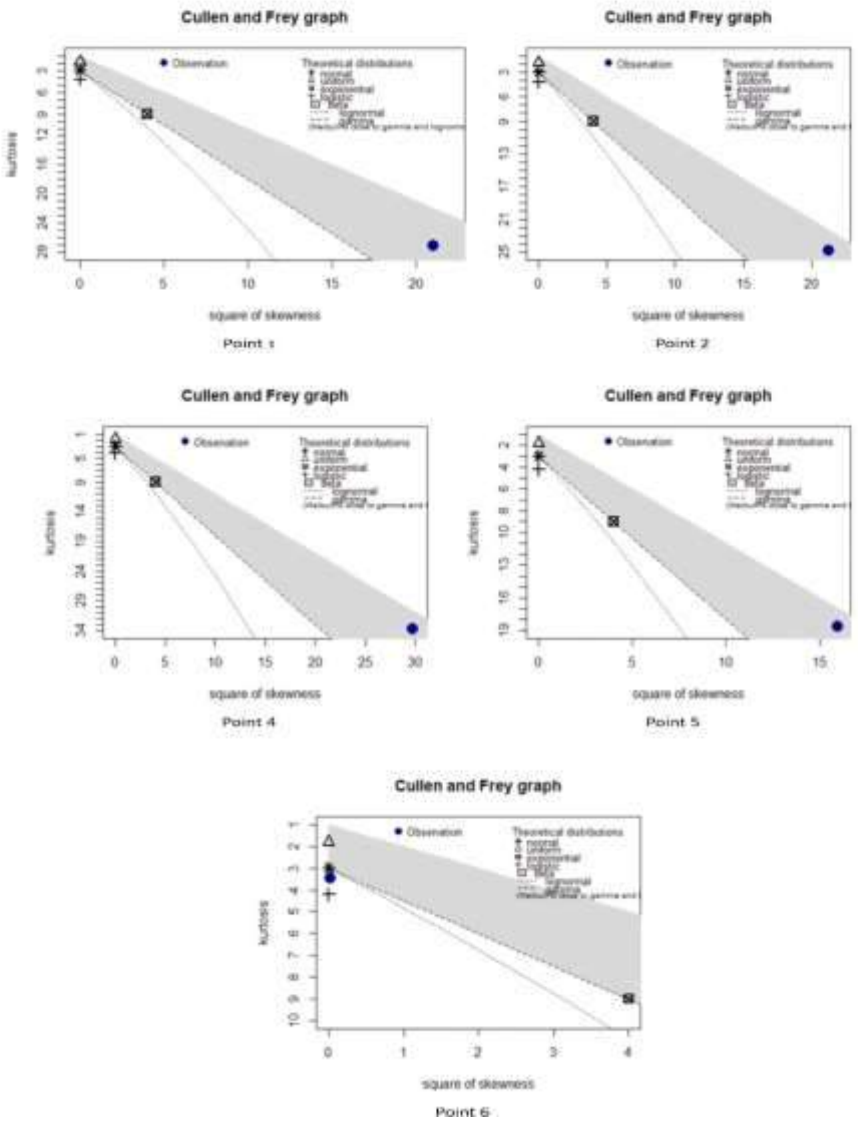

Figure 102. The Cullen and Frey diagrams for the distribution of Chl-a concentration at Points 1 - 6.

Table 21 presents the fitting parameters of the best-fit theoretical probability density function applied on the Chl-a concentration data extracted from Landsat in Ptelea lagoon. Mean and standard deviation parameters are given for the normal PDFs, log(mean) and log(sd) parameters for the log-normal distributions and shape and scale for the gamma distributions.

Table 21. Fitting parameters of the best-fit theoretical probability density function.

Points	**1**	**2**	**4**	**5**	**6**
Mean					1.218
St Dev					0.544
Log(Mean)		0.573	0.429	0.115	

Log(St Dev)		0.300	0.229	0.187	
Shape	1.593				
Scale	1.154				
LogLikelihood	-44.270	-89.803	-75.265	-57.250	-28.368
AIC	92.541	183.606	154.530	118.500	60.735
BIC	95.652	186.717	157.641	121.610	63.846

The theoretical probability density functions (PDFs) and the cumulative density functions (CDFs) applied as best-fit on the Chl-a data, together with the relevant Q-to-Q and P-to-P plots are shown in Figure 103.

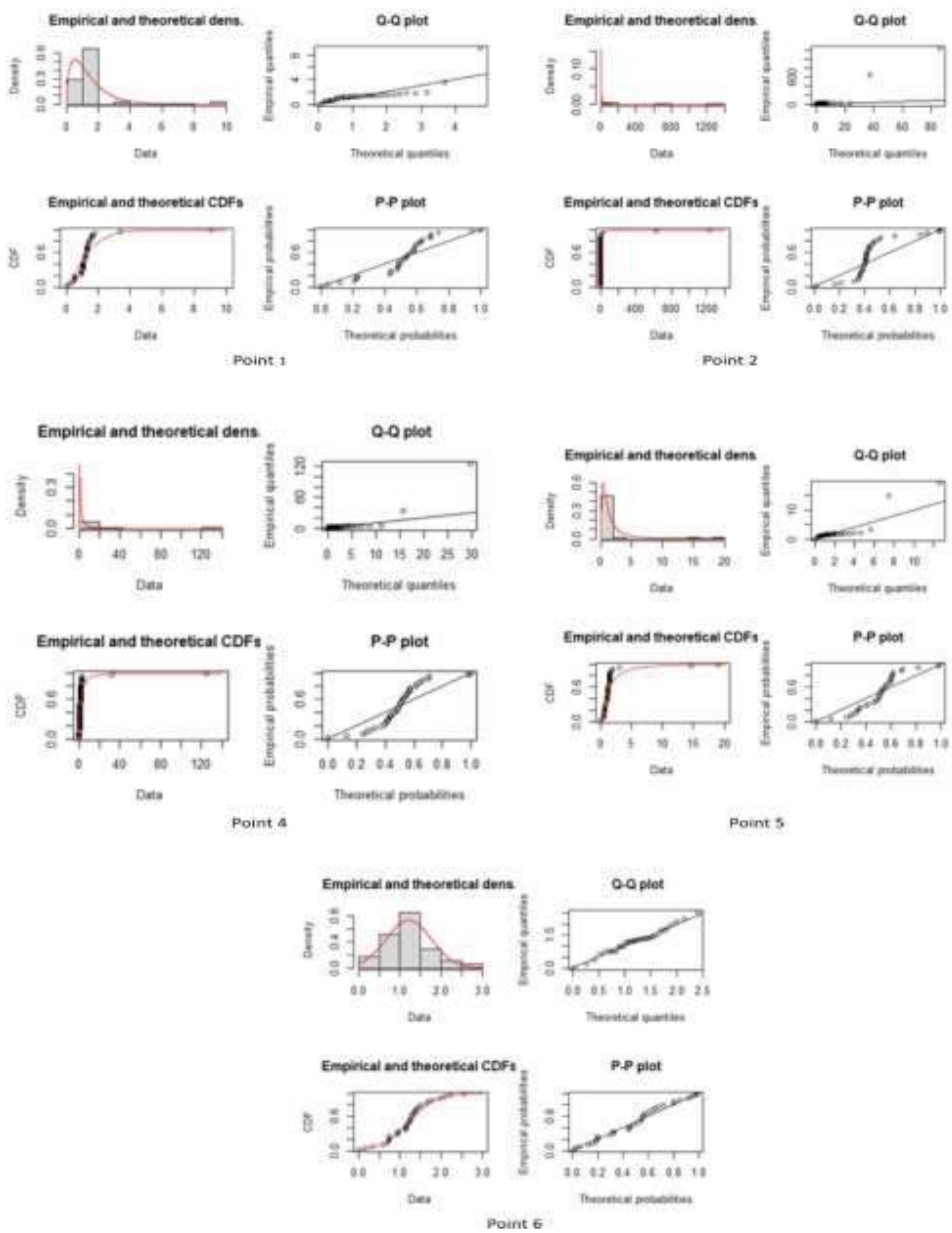

Figure 103. Theoretical probability density functions (PDFs) and the cumulative density functions (CDFs), applied as best-fit on the Chl-a data of points 1 – 6.

Based on the best-fit theoretical CDFs applied on the Chl-a, the probability of exceeding the eutrophication threshold of 2 μg/l was estimated. Probabilities of exceedance for all Ptelea lagoon points are summarized in Table 22 Probability is a measure that ranges between 0 and 1, with zero implying that eutrophication is impossible and 1 implying that eutrophication is absolutely certain.

Table 22. Probability of exceedance of the eutrophication threshold in Ptelea lagoon.

Points	Probability of Exceedance
1	0.645
2	0.473
4	0.423
5	0.301
6	0.075

Based on the above, points 1, 2 and 4 are more vulnerable to eutrophication effects than the rest of the lagoon. Exceedance probability is approx. 0.5, meaning that during half of a typical year eutrophication may exist. Based on the available Landsat images, it seems that the eutrophication prone periods are spring and summer. Point 6 has limited probability for a eutrophication event. Figure 104 illustrates the probability map of exceedance of the eutrophication threshold in Ptelea lagoon.

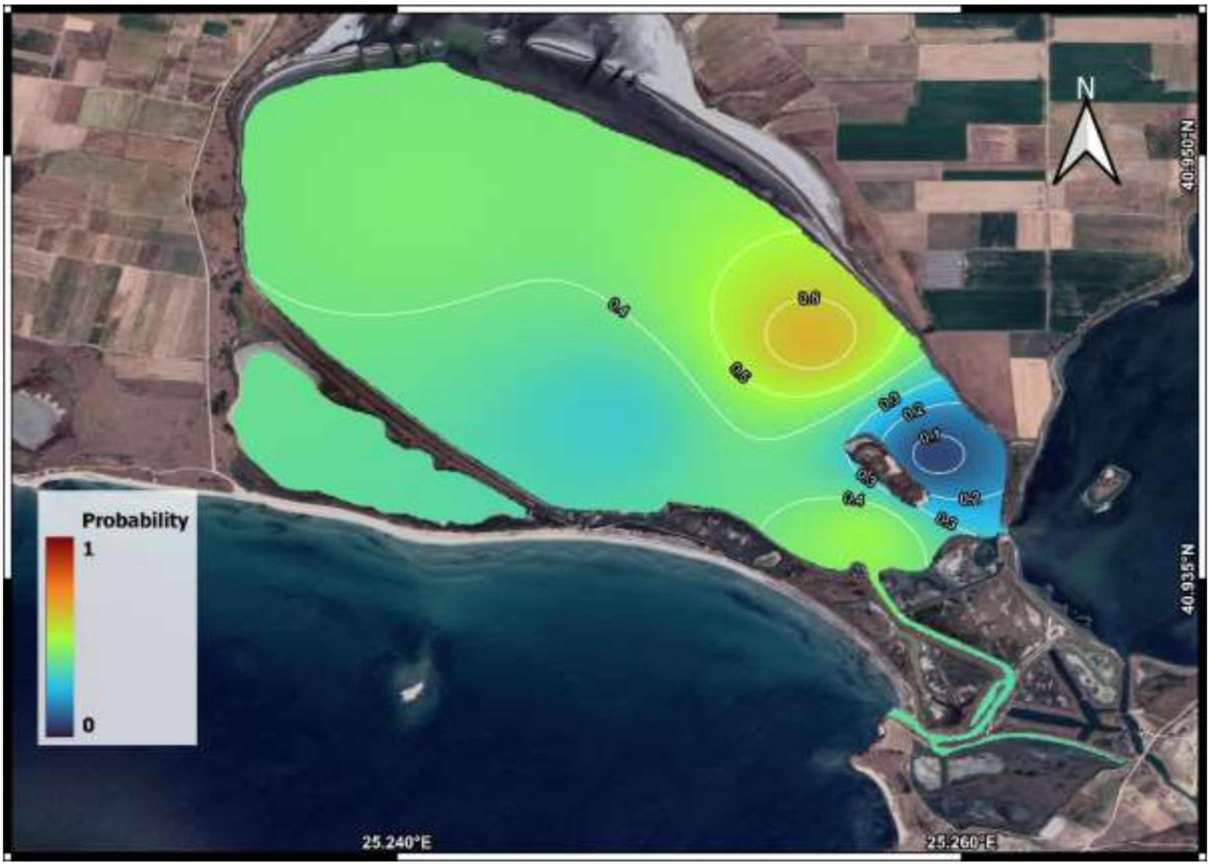

Figure 104. Probability map of exceedance of the eutrophication threshold in Ptelea lagoon.

3.2.2 Sentinel Data

3.2.2.1 Vassova lagoon

The points selected for Chl-a concentration extraction for the eutrophication assessment in Vassova lagoon, are the same as shown in Figure 75.

Table 23 presents the statistical measures for Chl-a concentration derived from Sentinel data at all points examined in Vassova lagoon.

Table 23. Statistical measures per point for Chl-a concentration at Vassova Lagoon.

Points	Min	Max	Median	Mean	St. deviation	Skewness	Kurtosis
1	0.149	37.452	1.802	2.400	4.418	7.918	66.740
2	0.084	5.165	1.912	1.941	0.677	1.448	10.598
3	0.408	4.661	2.189	2.161	0.730	0.500	4.790
4	0.086	7.966	3.322	3.318	1.359	0.367	4.689
5	0.440	241.690	2.116	5.984	29.548	8.052	68.175
6	0.115	3.893	2.125	2.143	0.533	-0.277	6.440
7	0.665	5.305	2.077	2.066	0.652	1.700	11.357

Figures 105 and 106 illustrate the skewness-kurtosis plot of Cullen and Frey for the Sentinel extracted Chl-a at all points in Vassova lagoon. Based on these graphs and the AIC and BIC criteria, it occurs that:

a) For Points 2, 3, 4 and 6, the normal distribution was found to be the best-fit theoretical distribution;
b) For Points 1, and 5, the log-normal distribution was found to be the best-fit theoretical distribution;
c) For Point 7, the gamma distribution was found to be the best-fit theoretical distribution.

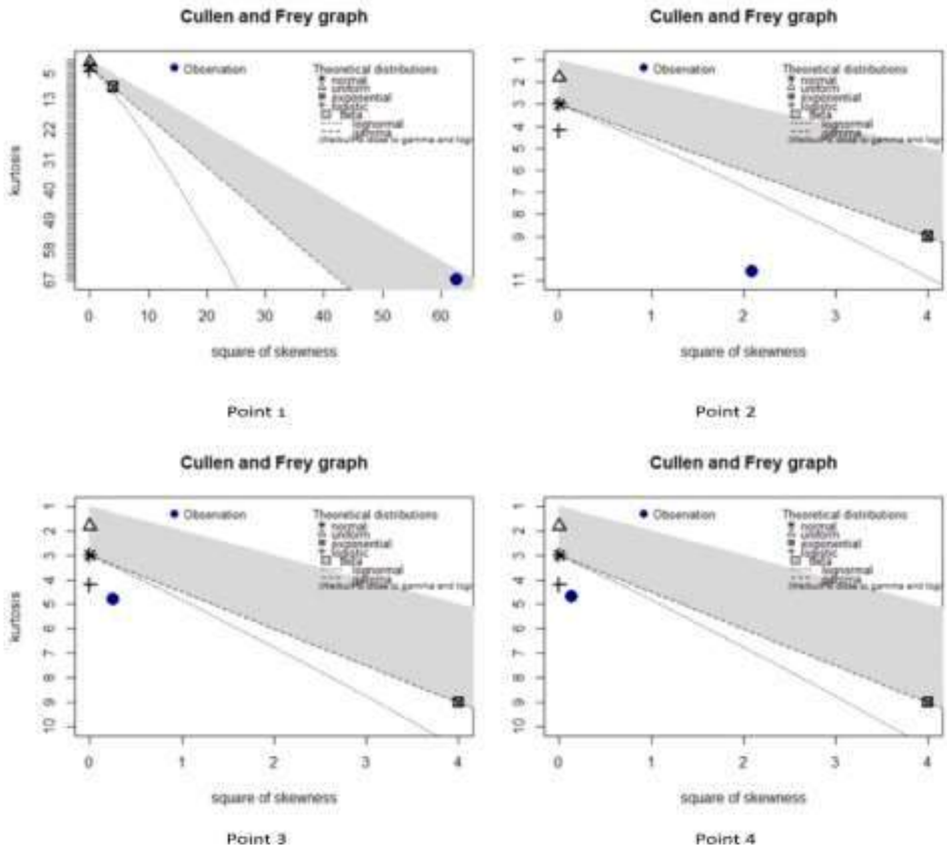

Figure 105. The Cullen and Frey diagrams for the distribution of Chl-a concentration at Points 1 - 4.

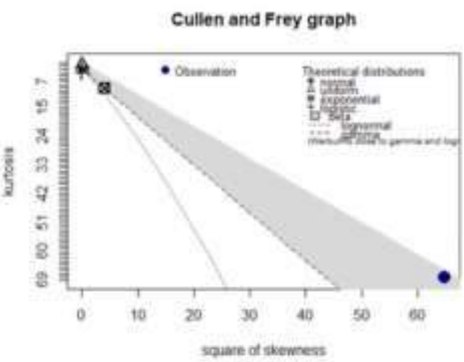

Point 5

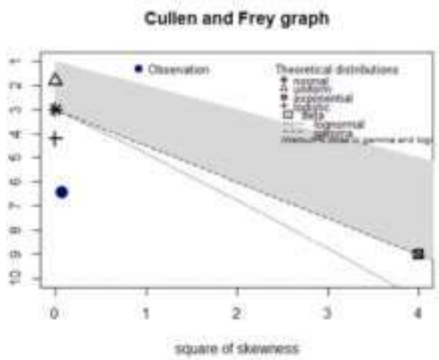

Point 6

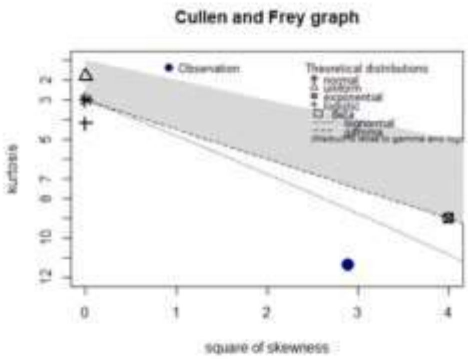

Point 7

Figure 106. The Cullen and Frey diagrams for the distribution of Chl-a concentration at Points 5 - 7.

Table 24 presents the fitting parameters of the best-fit theoretical probability density function applied on the Chl-a concentration data extracted from Sentinel in Vassova lagoon. Mean and standard deviation parameters are given for the normal PDFs, log(mean) and log(sd) parameters for the log-normal distributions and shape and scale for the gamma distributions.

Table 24. Fitting parameters of the best-fit theoretical probability density function.

Points	**1**	**2**	**3**	**4**	**5**	**6**	**7**
Mean		1.941	2.161	3.318		2.143	
St Dev		0.672	0.725	1.349		0.529	
Log(Mean)	0.605				0.793		
Log(St Dev)	0.068				0.089		
Shape							10.929
Scale							5.289
LogLikelihood	-94.750	-67.437	-72.401	-113.410	-124.785	-51.573	-60.575
AIC	193.500	138.873	148.801	230.821	253.569	107.146	125.149
BIC	197.879	143.252	153.181	235.200	257.949	111.525	129.529

The theoretical probability density functions (PDFs) and the cumulative density functions (CDFs) applied as best-fit on the Chl-a data, together with the relevant Q-to-Q and P-to-P plots are shown in Figures 107 and 108.

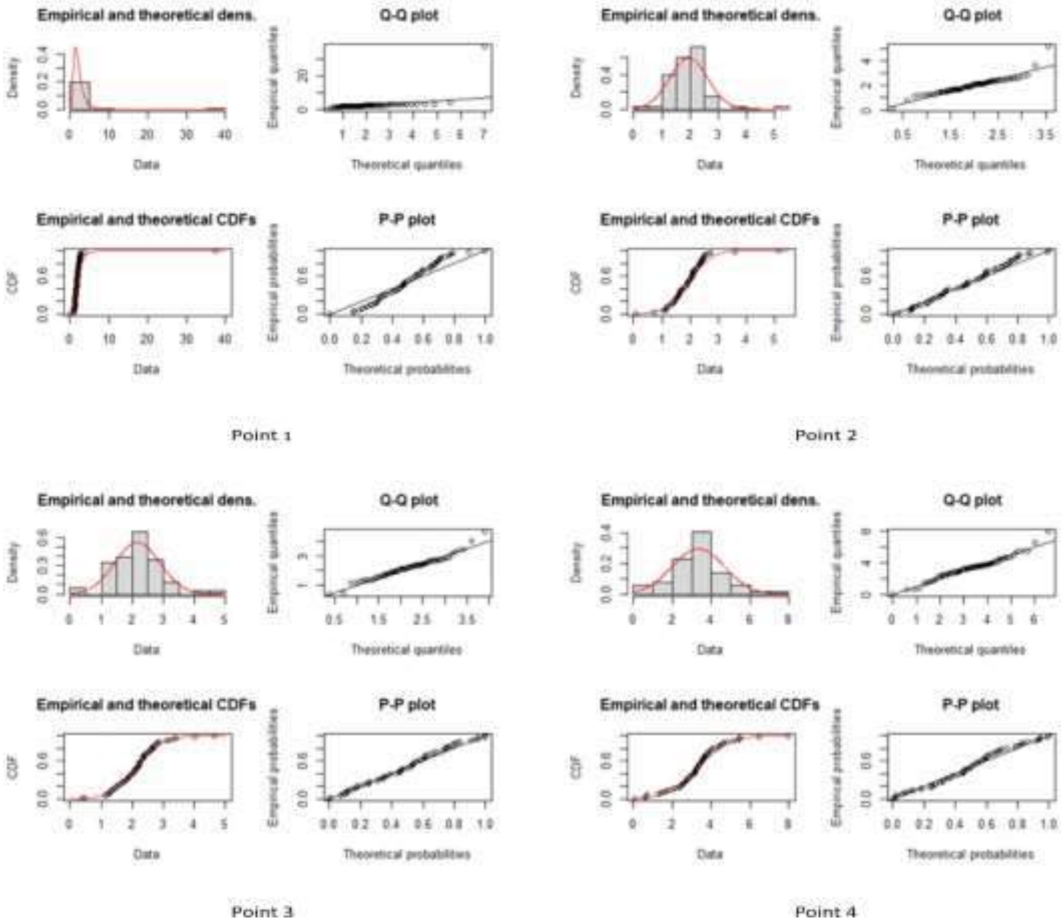

Figure 107. Theoretical probability density functions (PDFs) and the cumulative density functions (CDFs), applied as best-fit on the Chl-a data of points 1 – 4.

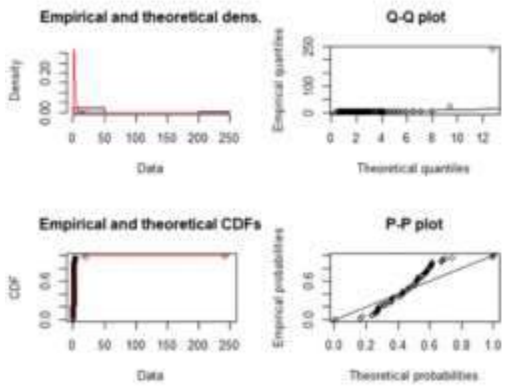

Point 5

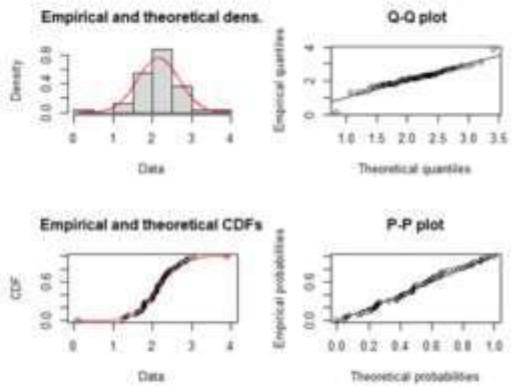

Point 6

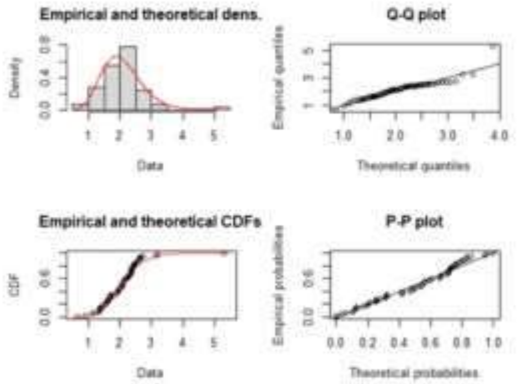

Point 7

Figure 108. Theoretical probability density functions (PDFs) and the cumulative density functions (CDFs), applied as best-fit on the Chl-a data of points 5 – 7.

Based on the best-fit theoretical CDFs applied on the Chl-a, the probability of exceeding the eutrophication threshold of 2 μg/l was estimated. Probabilities of exceedance for all Vassova lagoon points are summarized in Table 25. Probability is a measure that ranges between 0 and 1, with zero implying that eutrophication is impossible and 1 implying that eutrophication is absolutely certain. Figure 109 illustrates the probability map of exceedance of the eutrophication threshold in Vassova lagoon.

Table 25. Probability of exceedance of the eutrophication threshold in Vassova lagoon.

Points	**Probability of Exceedance**
1	0.437
2	0.465
3	0.588
4	0.836
5	0.554
6	0.607
7	0.502

Based on the above, all points are more vulnerable to eutrophication effects. For point 4, exceedance probability is approximately 0.8 meaning that almost ten months of the year eutrophication may exist. Points 1 and 2 show the lower exceedance probability, below 0.5. Based on the available Sentinel images, it seems that the eutrophication prone periods are spring and summer.

Figure 109. Probability map of exceedance of the eutrophication threshold in Vassova lagoon.

3.2.2.2 Eratino lagoon

The points selected for Chl-a concentration extraction for the eutrophication assessment in Eratino lagoon, are shown in Figure 110. These points cover the typical conditions at all sub-basins of the lagoon and are distributed among various depths.

Figure 110. Points for Chl-a concentration extraction in Eratino lagoon.

Table 26 presents the statistical measures for Chl-a concentration at all points examined in Eratino lagoon.

Table 26. Statistical measures per point for Chl-a concentration at Eratino Lagoon.

Points	Min	Max	Median	Mean	St. deviation	Skewness	Kurtosis
1	0.090	3.272	2.070	2.101	0.506	-0.849	5.972
2	0.985	4.875	1.609	1.752	0.640	2.395	11.850
3	0.591	5.110	2.038	2.091	0.613	1.595	11.805
4	1.049	6.015	2.113	2.259	0.855	1.561	7.631
5	0.800	23.254	1.831	2.133	2.789	7.249	58.347
6	0.021	4.011	2.010	1.989	0.620	0.103	6.094
7	0.111	49.525	2.177	2.865	6.006	7.806	64.592
8	0.553	5.243	2.618	2.689	0.819	0.722	4.491
9	0.842	7.833	1.746	1.813	0.910	4.753	34.156

Figures 111 and 112 illustrate the skewness-kurtosis plot of Cullen and Frey for the Sentinel extracted Chl-a at all points in Eratino lagoon. Based on these graphs and the AIC and BIC criteria, it occurs that:

a) For Points 1 and 6, the normal distribution was found to be the best-fit theoretical distribution;
b) For Points 5, 7 and 9, the log-normal distribution was found to be the best-fit theoretical distribution;
c) For Points 3 and 8, the gamma distribution was found to be the best-fit theoretical distribution;
d) For Points 2 and 3, the gumbel distribution was found to be the best-fit theoretical distribution.

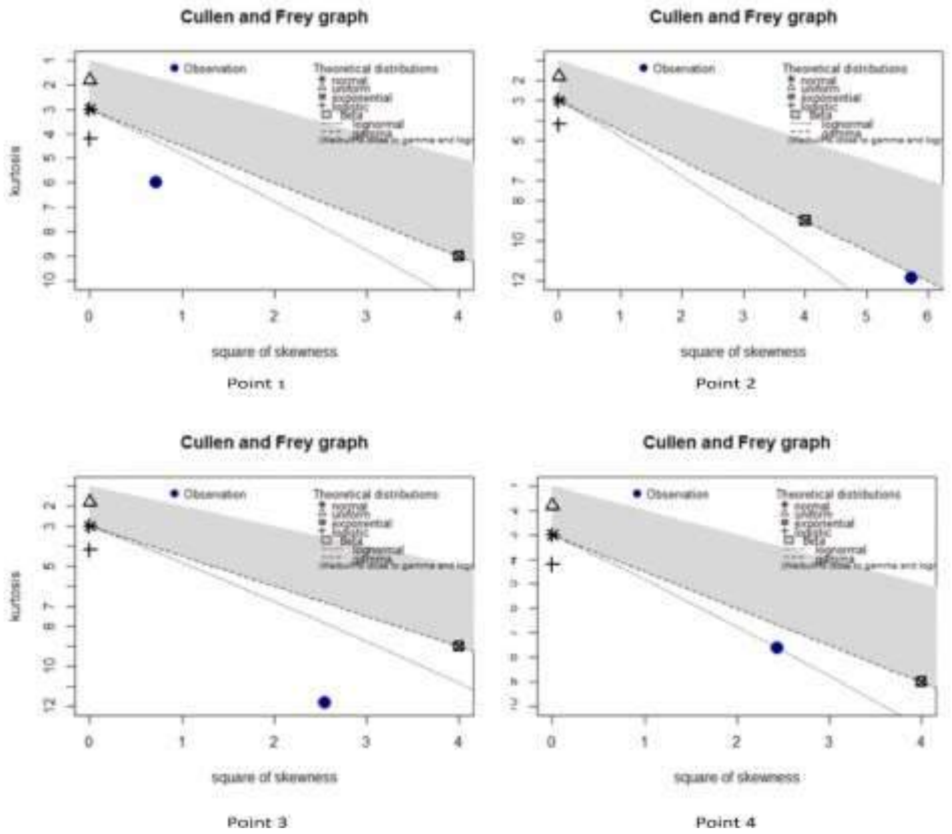

Figure 111. The Cullen and Frey diagrams for the distribution of Chl-a concentration at Points 1 - 4.

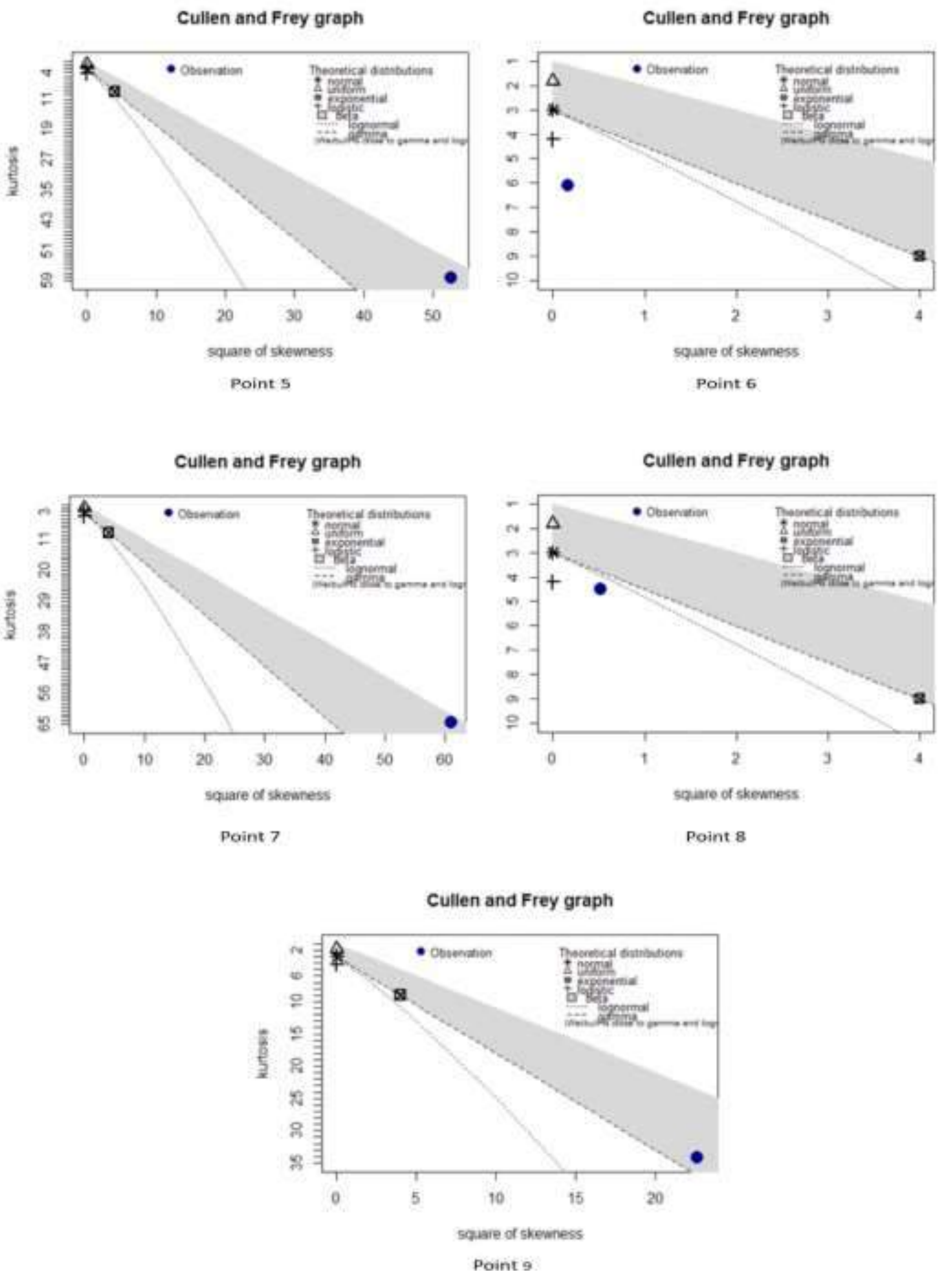

Figure 112. The Cullen and Frey diagrams for the distribution of Chl-a concentration at Points 5 - 9.

Table 27 presents the fitting parameters of the best-fit theoretical probability density function applied on the Chl-a concentration data extracted from Sentinel in Eratino lagoon. Mean and standard deviation parameters are given for the normal PDFs, log(mean) and log(sd) parameters for the log-normal distributions and shape and scale for the gamma distributions.

Table 27. Fitting parameters of the best-fit theoretical probability density function.

Points	**1**	**2**	**3**	**4**	**5**	**6**	**7**	**8**	**9**
Mean	2.101					1.988			
St Dev	0.502					0.615			
Log(Mean)					0.567		0.730		0.522
Log(St Dev)					0.058		0.077		0.045
Shape			12.047					10.316	
Scale			5.761					3.836	
a		1.499		1.890					
b		0.400		0.617					
LogLikelihood	-45.924	-45.074	-55.689	-70.247	-76.641	-58.811	-104.135	-76.120	-56.811
AIC	95.849	94.149	115.378	144.495	157.283	121.623	212.270	156.240	117.621
BIC	100.135	98.435	119.665	148.781	161.569	125.909	216.556	160.526	121.908

The theoretical probability density functions (PDFs) and the cumulative density functions (CDFs) applied as best-fit on the Chl-a data, together with the relevant Q-to-Q and P-to-P plots are shown in Figures 113 and 114.

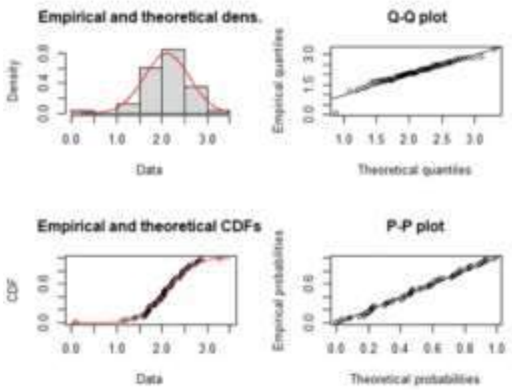

Point 1

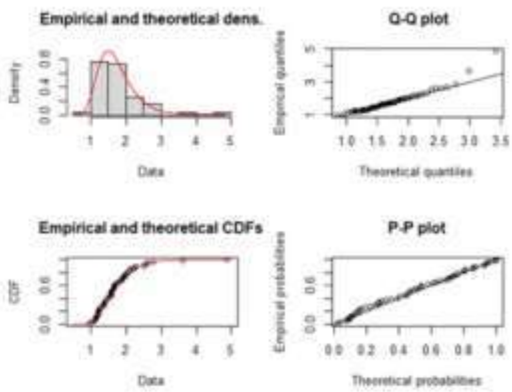

Point 2

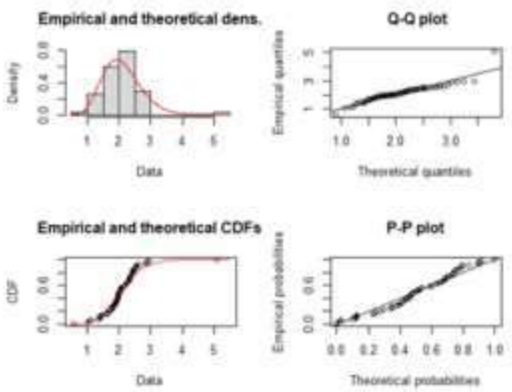

Point 3

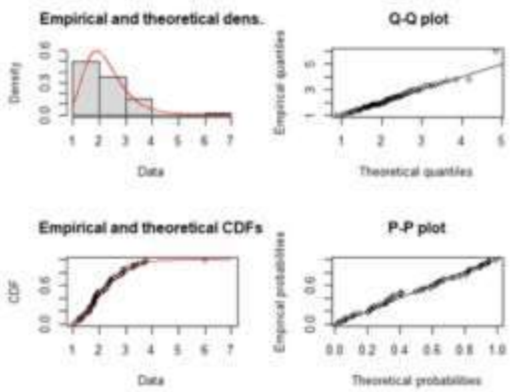

Point 4

Figure 113. Theoretical probability density functions (PDFs) and the cumulative density functions (CDFs), applied as best-fit on the Chl-a data of points 1 – 4.

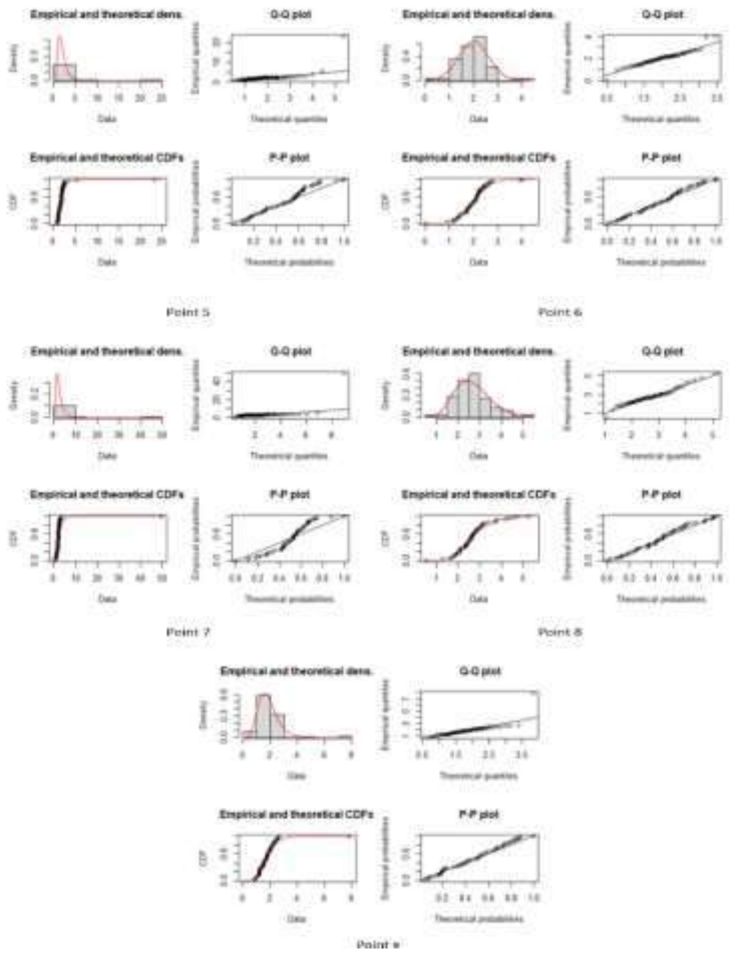

Figure 114. Theoretical probability density functions (PDFs) and the cumulative density functions (CDFs), applied as best-fit on the Chl-a data of points 5 – 9.

Based on the best-fit theoretical CDFs applied on the Chl-a, the probability of exceeding the eutrophication threshold of 2 μg/l was estimated. Probabilities of exceedance for all Eratino lagoon points are summarized in Table 28. Probability is a measure that ranges between 0 and 1, with zero implying that eutrophication is impossible and 1 implying that eutrophication is absolutely certain. Figure 115 illustrates the probability map of exceedance of the eutrophication threshold in Eratino lagoon.

Table 28. Probability of exceedance of the eutrophication threshold in Eratino lagoon.

Points	**Probability of Exceedance**
1	0.580
2	0.273
3	0.523

4	0.568
5	0.393
6	0.492
7	0.524
8	0.802
9	0.348

Based on the above, points 1, 3, 4, 6, 7 and 8 are more vulnerable to eutrophication effects. Point 1 is close to the inlet of the lagoon, point 4 in the natural channel which supply the lagoon with agricultural runoff, point 3 is in the upper part of the lagoon and points 6, 7 and 8 in the east part of the lagoon. For points 1, 3, 4, 6 and 7, exceedance probability is approximately 0.5 and for point 8 is higher reaching 0.8. Points 2, 5 and 9 have limited probability for a eutrophication event.

Figure 115. Probability map of exceedance of the eutrophication threshold in Eratino lagoon.

3.2.2.3 Agiasma lagoon

The points selected for Chl-a concentration extraction for the eutrophication assessment in Agiasma lagoon, are shown in Figure 81.

Table 29 presents the statistical measures for Chl-a concentration at all points examined in Agiasma lagoon.

Table 29. Statistical measures per point for Chl-a concentration at Agiasma Lagoon.

Points	Min	Max	Median	Mean	St. deviation	Skewness	Kurtosis
1	0.919	6.572	1.753	1.926	0.842	3.107	17.261
2	0.882	5.090	1.939	2.023	0.617	2.034	11.505
3	1.301	7.467	1.990	2.231	0.961	3.547	17.863
4	1.026	5.742	2.240	2.272	0.754	1.837	9.836
5	0.916	5.236	1.933	2.058	0.889	1.947	7.850
6	0.410	222.925	2.078	5.522	26.618	8.250	71.347
7	0.815	13.700	1.668	1.864	1.546	6.783	55.045
8	1.014	15.508	2.461	2.638	1.776	5.773	44.357

Figures 116 and 117 illustrate the skewness-kurtosis plot of Cullen and Frey for the Sentinel extracted Chl-a at all points in Agiasma lagoon. Based on these graphs and the AIC and BIC criteria, it occurs that:

a) For Points 1, 2, 3, 4, 6, 7 and 8, the log-normal distribution was found to be the best-fit theoretical distribution;

b) For Point 5, the gamma distribution was found to be the best-fit theoretical distribution.

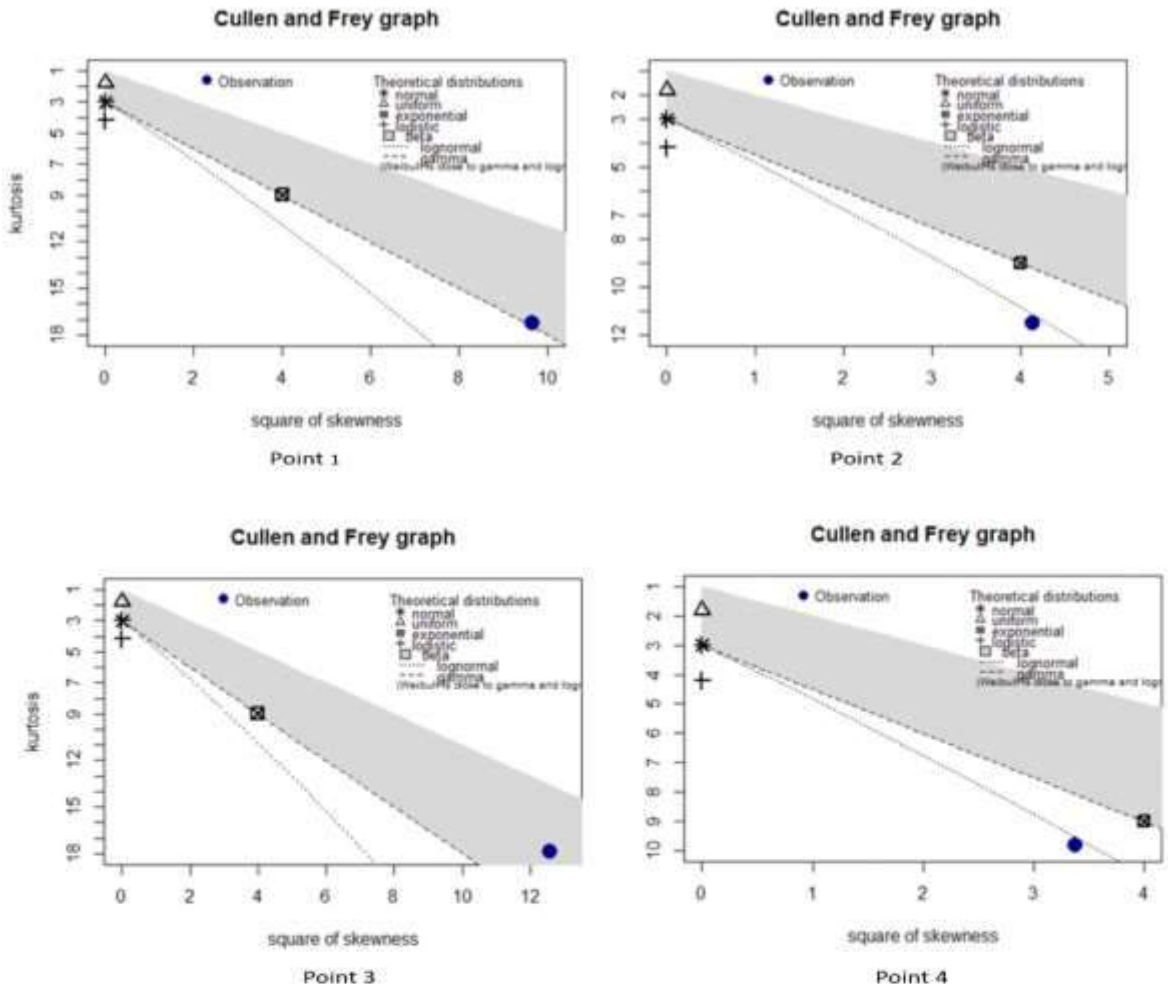

Figure 116. The Cullen and Frey diagrams for the distribution of Chl-a concentration at Points 1 - 4.

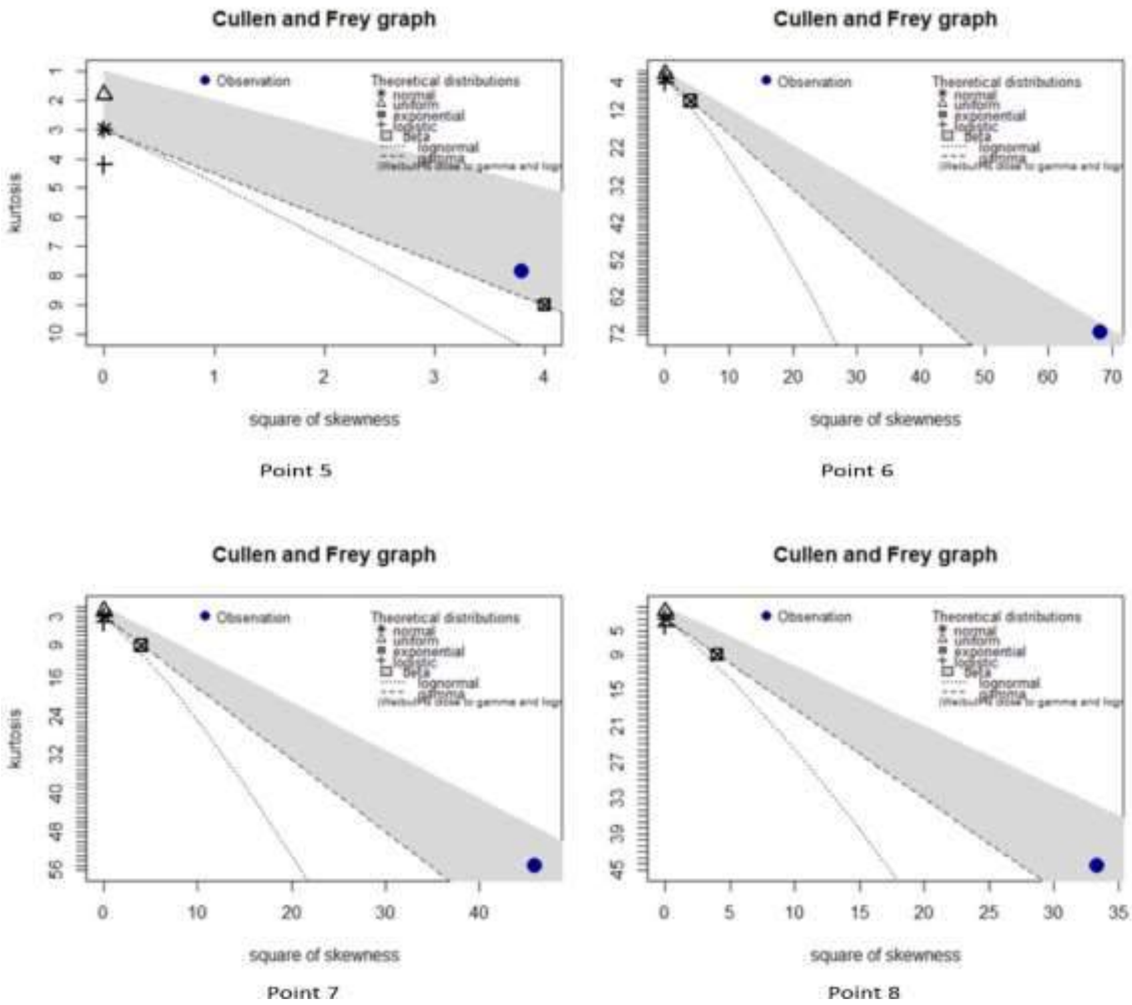

Figure 117. The Cullen and Frey diagrams for the distribution of Chl-a concentration at Points 5 - 8.

Table 30 presents the fitting parameters of the best-fit theoretical probability density function applied on the Chl-a concentration data extracted from Sentinel in Agiasma lagoon. Mean and standard deviation parameters are given for the normal PDFs, log(mean) and log(sd) parameters for the log-normal distributions and shape and scale for the gamma distributions.

Table 30. Fitting parameters of the best-fit theoretical probability density function.

Points	**1**	**2**	**3**	**4**	**5**	**6**	**7**	**8**
Mean								
St Dev								
Log(Mean)	0.590	0.665	0.747	0.773		0.775	0.505	0.866
Log(St Dev)	0.041	0.033	0.036	0.037		0.088	0.049	0.050
Shape					6.925			
Scale					3.365			

LogLikelihood	-64.474	-55.335	-65.869	-69.757	-77.509	-130.029	-70.913	-96.403
AIC	132.949	114.670	135.738	143.514	159.017	264.058	145.826	196.805
BIC	137.417	119.138	140.207	147.982	163.485	268.526	150.294	201.273

The theoretical probability density functions (PDFs) and the cumulative density functions (CDFs) applied as best-fit on the Chl-a data, together with the relevant Q-to-Q and P-to-P plots are shown in Figures 118 and 119.

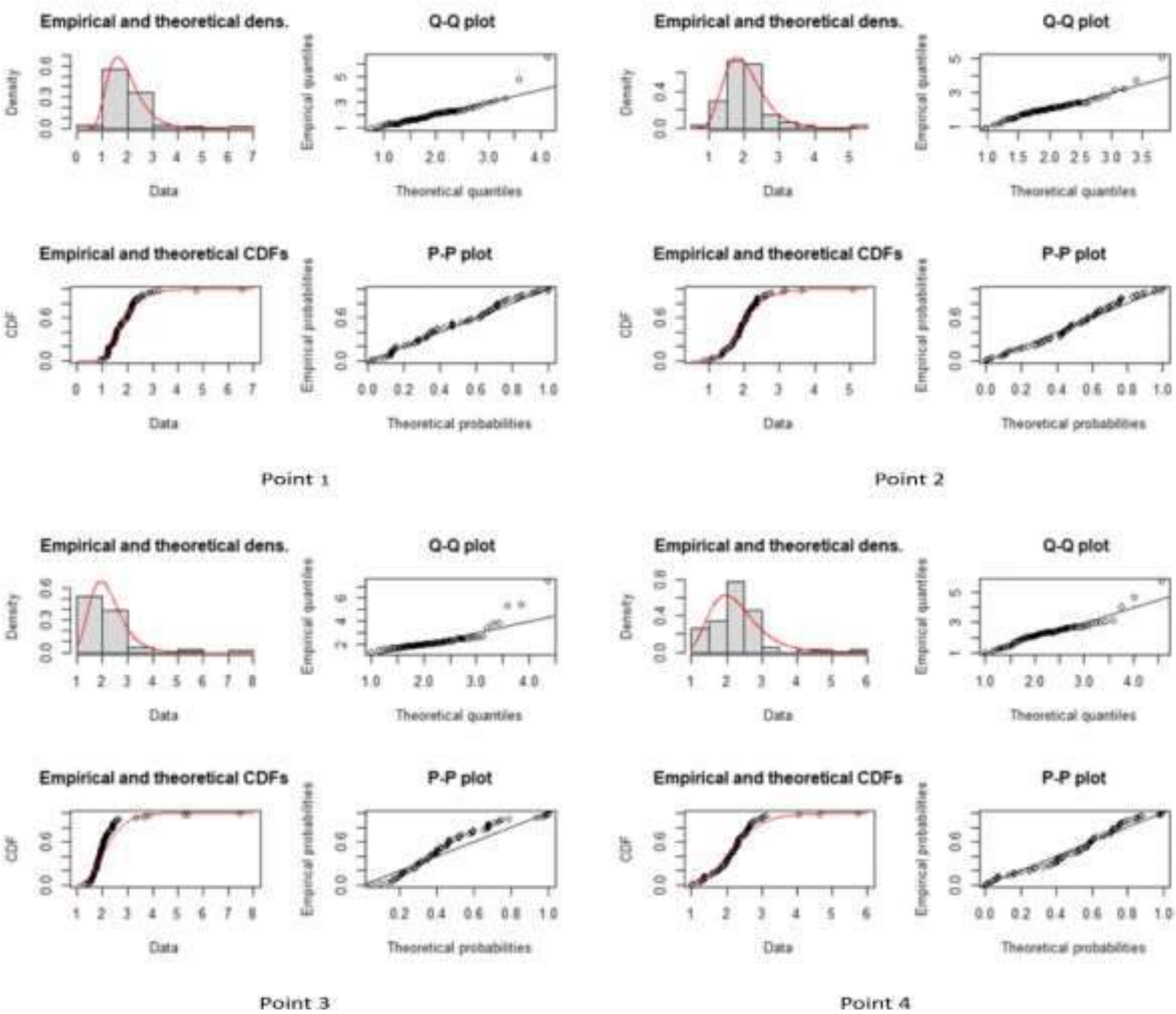

Figure 118. Theoretical probability density functions (PDFs) and the cumulative density functions (CDFs), applied as best-fit on the Chl-a data of points 1 – 4.

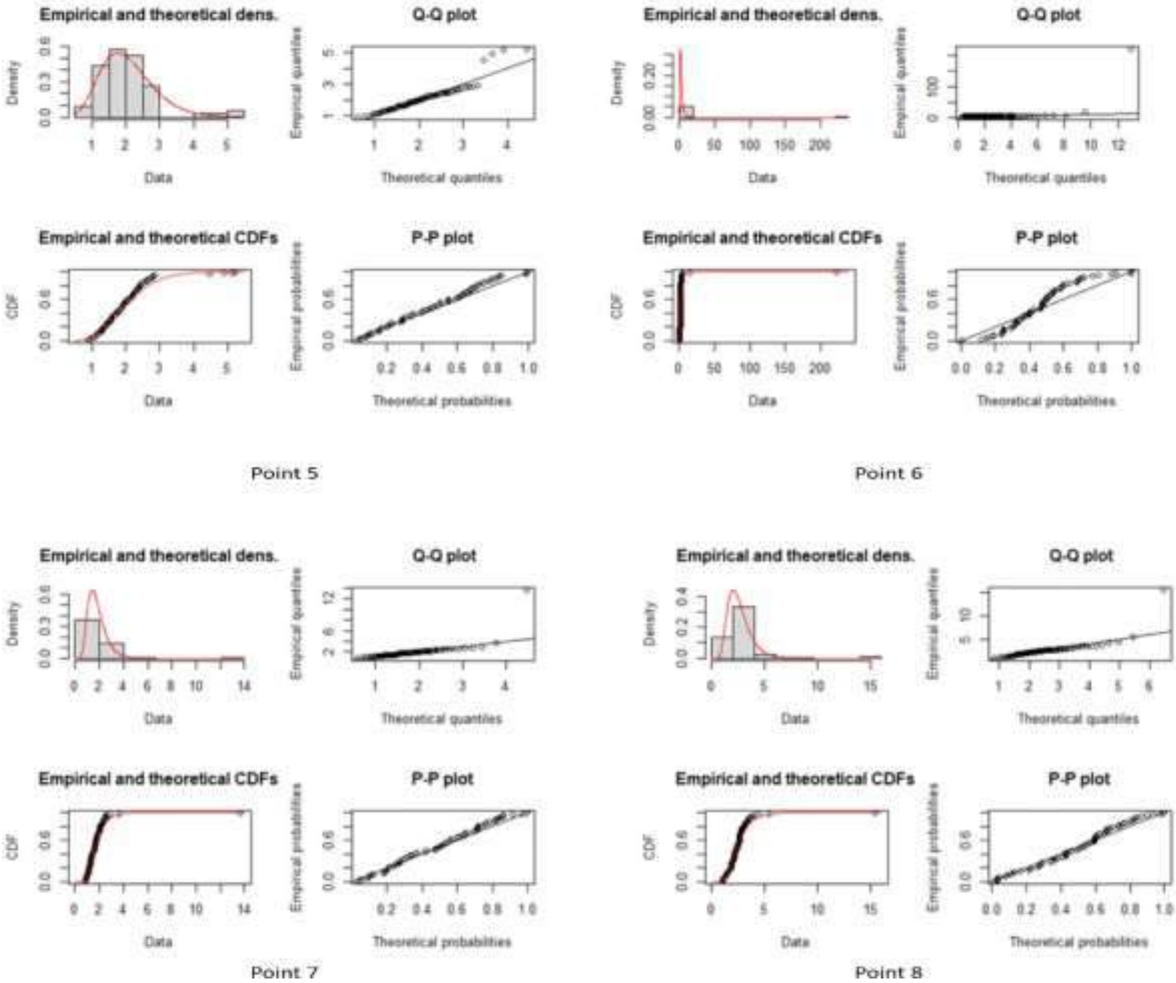

Figure 119. Theoretical probability density functions (PDFs) and the cumulative density functions (CDFs), applied as best-fit on the Chl-a data of points 5 – 8.

Based on the best-fit theoretical CDFs applied on the Chl-a, the probability of exceeding the eutrophication threshold of 2 μg/l was estimated. Probabilities of exceedance for all Agiasma lagoon points are summarized in Table 31. Probability is a measure that ranges between 0 and 1, with zero implying that eutrophication is impossible and 1 implying that eutrophication is absolutely certain. Figure 120 illustrates the probability map of exceedance of the eutrophication threshold in Agiasma lagoon.

Table 31. Probability of exceedance of the eutrophication threshold in Agiasma lagoon.

Points	Probability of Exceedance
1	0.381
2	0.460
3	0.572
4	0.602
5	0.479
6	0.544

7	0.322
8	0.662

Based on the above, points 3, 4, 6 and 86 are more vulnerable to eutrophication effects with exceedance probability over 0.5 and points 2 and 5 follows with exceedance probability a little lower than 0.5. Points 2, 3 and 8 are located in the lower part of the lagoon and close to the lagoon inlet. Points 1 and 7 have limited probability for a eutrophication event.

Figure 120. Probability map of exceedance of the eutrophication threshold in Eratino lagoon.

3.2.2.4 Porto Lagos lagoon

The points selected for Chl-a concentration extraction for the eutrophication assessment in Porto Lagos lagoon, are shown in Figure 87.

Table 32 presents the statistical measures for Chl-a concentration at all points examined in Porto Lagos lagoon.

Table 32. Statistical measures per point for Chl-a concentration at Porto Lagos lagoon.

Points	Min	Max	Median	Mean	St. deviation	Skewness	Kurtosis
1	0.913	19.864	1.818	2.180	2.331	6.959	55.819
2	0.854	6.520	2.050	2.076	0.725	3.581	24.236
3	0.894	2.856	1.775	1.789	0.426	0.212	2.453

4	0.323	16.440	1.510	1.915	2.000	6.257	47.292
5	0.567	214.846	1.647	5.802	27.048	7.437	60.297
6	0.697	68.272	1.693	3.275	8.436	7.310	59.390
7	0.691	1094.969	1.783	18.410	134.557	8.124	68.994
8	0.668	831.726	1.610	14.807	102.143	8.114	68.891
9	0.520	84.250	1.468	2.868	10.204	8.047	68.133
10	0.672	14.246	1.409	1.760	1.699	6.396	49.374
11	0.633	68.025	1.430	2.684	8.221	7.962	67.178
12	0.816	4.392	1.440	1.679	0.774	1.620	5.995
13	0.066	4.358	0.789	1.050	0.882	1.344	5.089

Figures 121, 122 and 123 illustrate the skewness-kurtosis plot of Cullen and Frey for the Sentinel extracted Chl-a at all points in Porto Lagos lagoon. Based on these graphs and the AIC and BIC criteria, it occurs that:

a) For Points 1, 5, 6, 7, 8, 9, 10. 11 and 12, the log-normal distribution was found to be the best-fit theoretical distribution;
b) For Point 3 and 13, the gamma distribution was found to be the best-fit theoretical distribution;
c) For Points 2 and 4, the gumbel distribution was found to be the best-fit theoretical distribution.

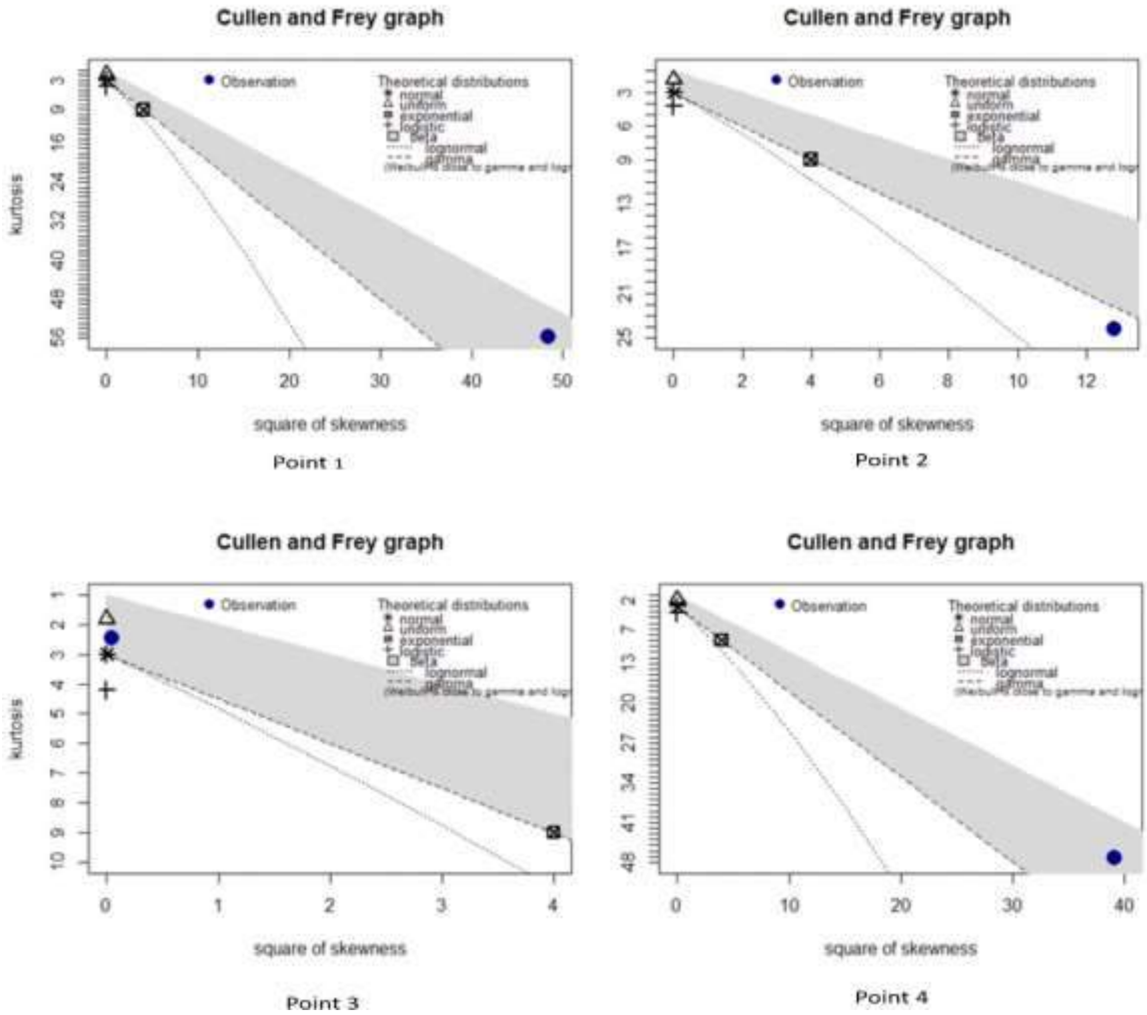

Figure 121. The Cullen and Frey diagrams for the distribution of Chl-a concentration at Points 1 - 4.

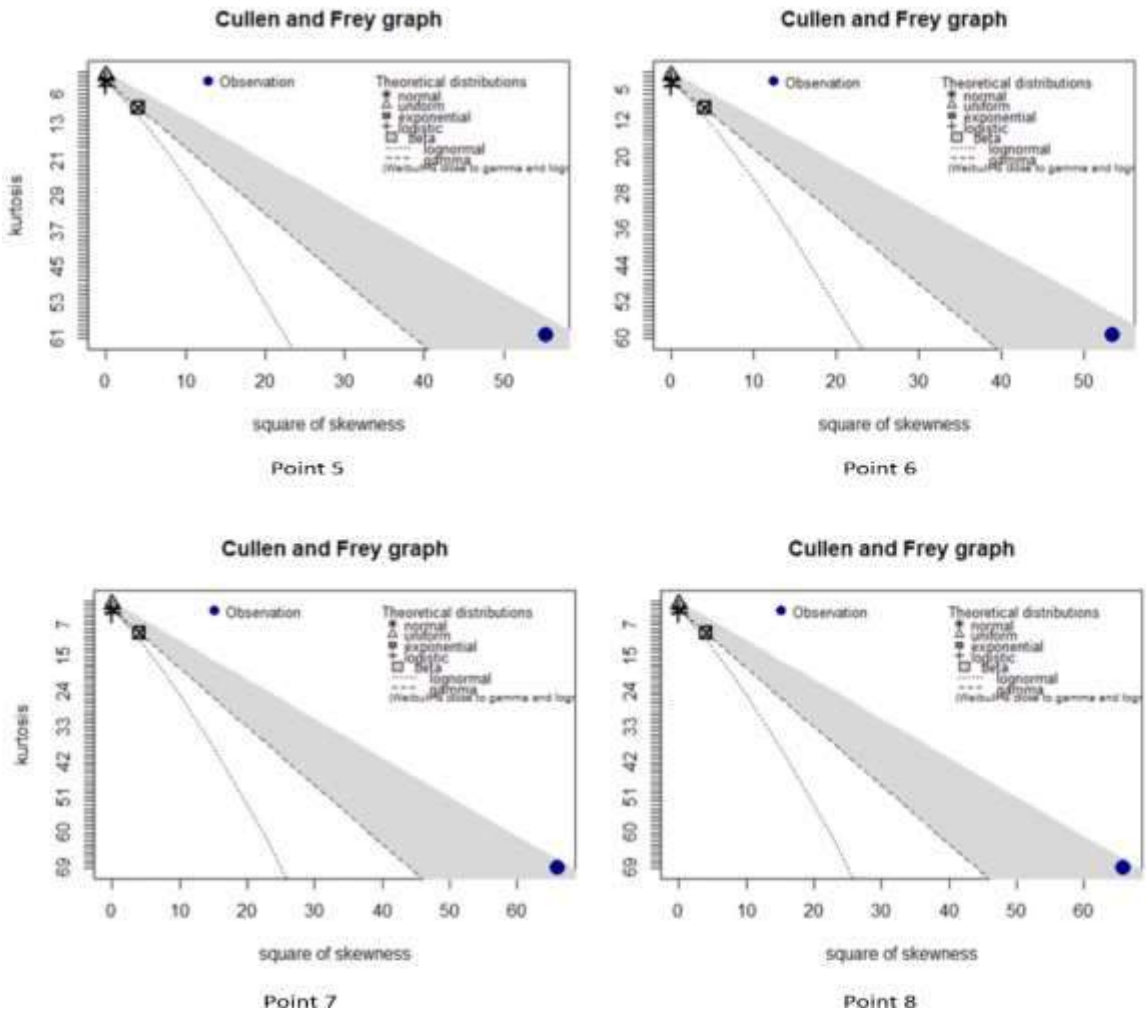

Figure 122. The Cullen and Frey diagrams for the distribution of Chl-a concentration at Points 5 - 8.

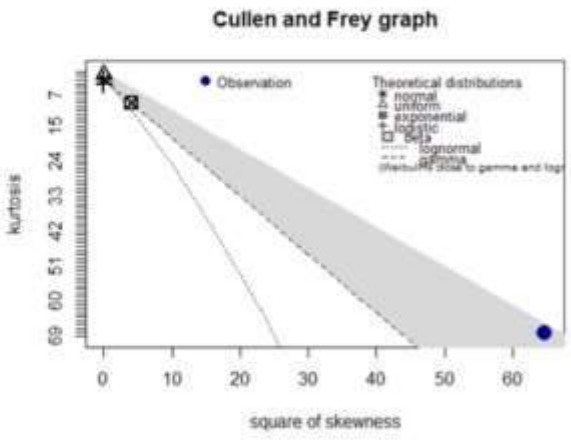

Point 9

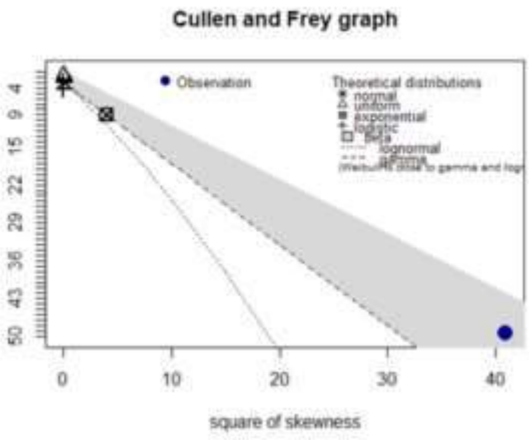

Point 10

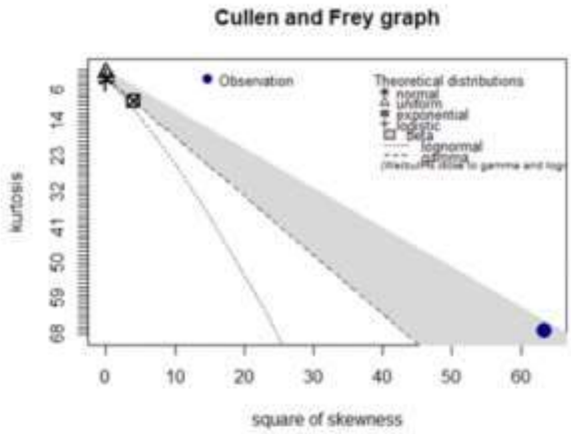

Point 11

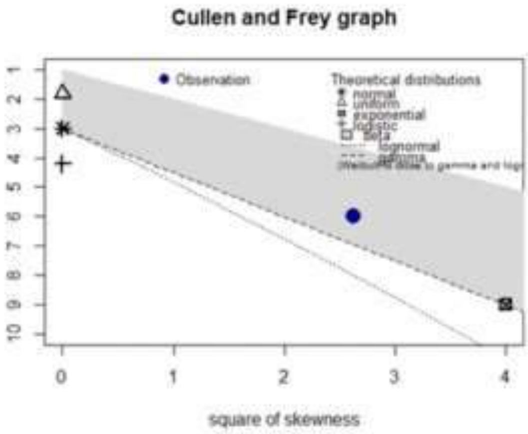

Point 12

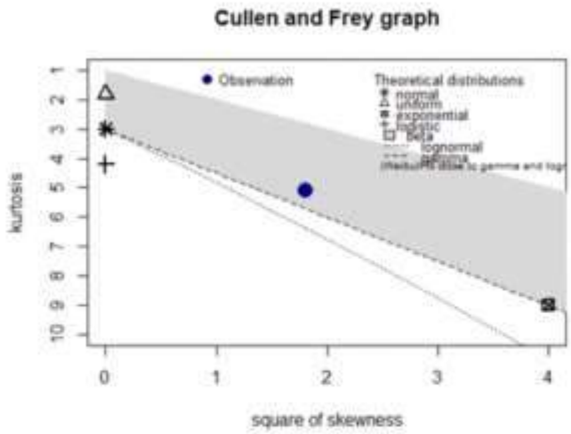

Point 13

Figure 123. The Cullen and Frey diagrams for the distribution of Chl-a concentration at Points 9 - 13.

Table 33 presents the fitting parameters of the best-fit theoretical probability density function applied on the Chl-a concentration data extracted from Landsat in Porto Lagos lagoon. Mean and standard deviation parameters are given for the normal PDFs, log(mean) and log(sd) parameters for the log-normal distributions and shape and scale for the gamma distributions.

Table 33. Fitting parameters of the best-fit theoretical probability density function.

Points	**1**	**2**	**3**	**4**	**5**	**6**	**7**
Mean							
St Dev							
Log(Mean)	0.621				0.613	0.678	0.622
Log(St Dev)	0.055				0.100	0.084	0.110
Shape			17.465				
Scale			9.760				
a		1.803		1.433			
b		0.475		0.671			
LogLikelihood	-81.529	-54.843	-36.387	-87.002	-119.745	-112.870	-127.103
AIC	167.184	113.686	76.774	178.003	243.489	229.740	258.205
BIC	171.654	118.066	81.153	182.382	247.868	234.119	262.584
Points	**8**	**9**	**10**	**11**	**12**	**13**	
Mean							
St Dev							
Log(Mean)	0.641	0.454	0.414	0.470	0.431		
Log(St Dev)	0.117	0.078	0.556	0.076	0.050		
Shape						1.215	
Scale							
a							
b							
LogLikelihood	-132.631	-93.181	-68.540	-94.151	-62.039	-67.317	
AIC	269.262	190.362	141.079	192.303	128.079	138.632	
BIC	273.641	194.741	145.459	196.682	132.458	143.012	

The theoretical probability density functions (PDFs) and the cumulative density functions (CDFs) applied as best-fit on the Chl-a data, together with the relevant Q-to-Q and P-to-P plots are shown in Figures 124, 125 and 126.

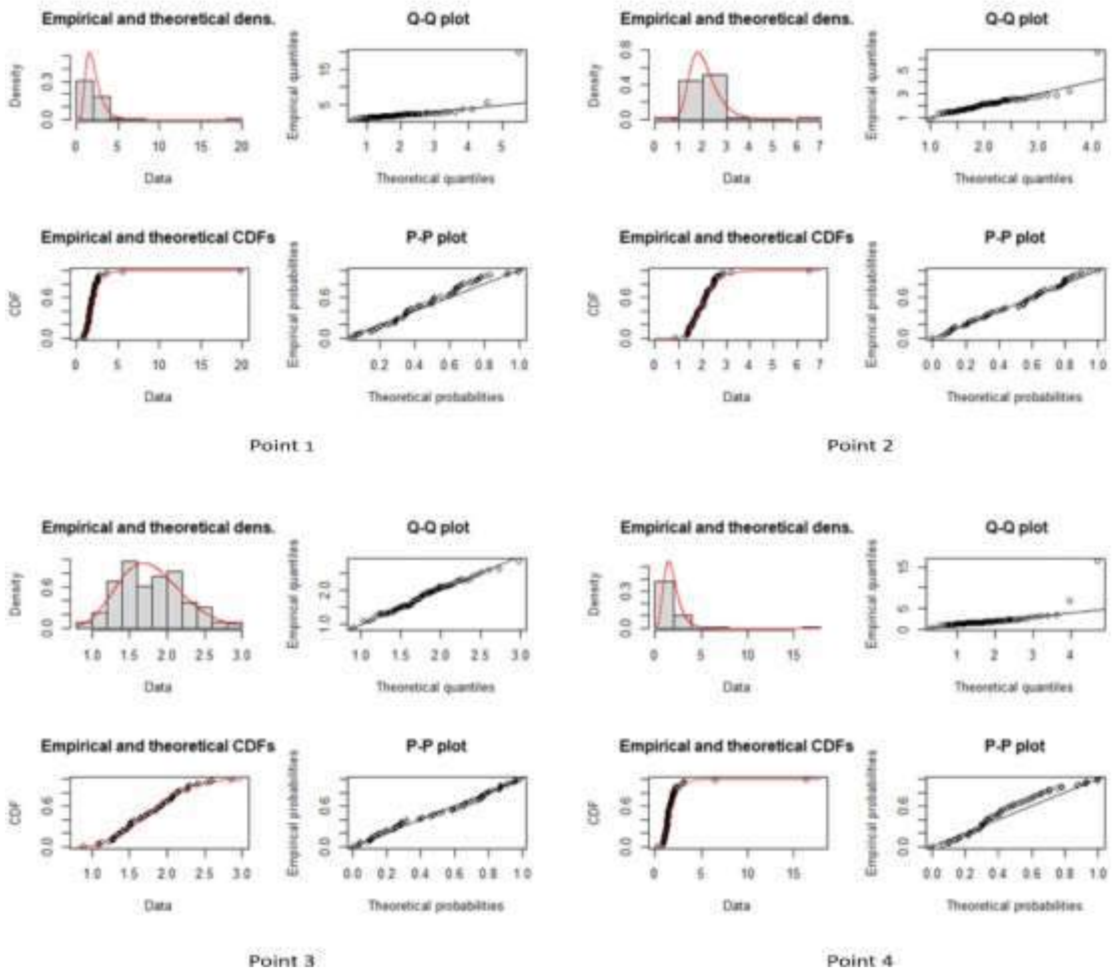

Figure 124. Theoretical probability density functions (PDFs) and the cumulative density functions (CDFs), applied as best-fit on the Chl-a data of points 1 - 4.

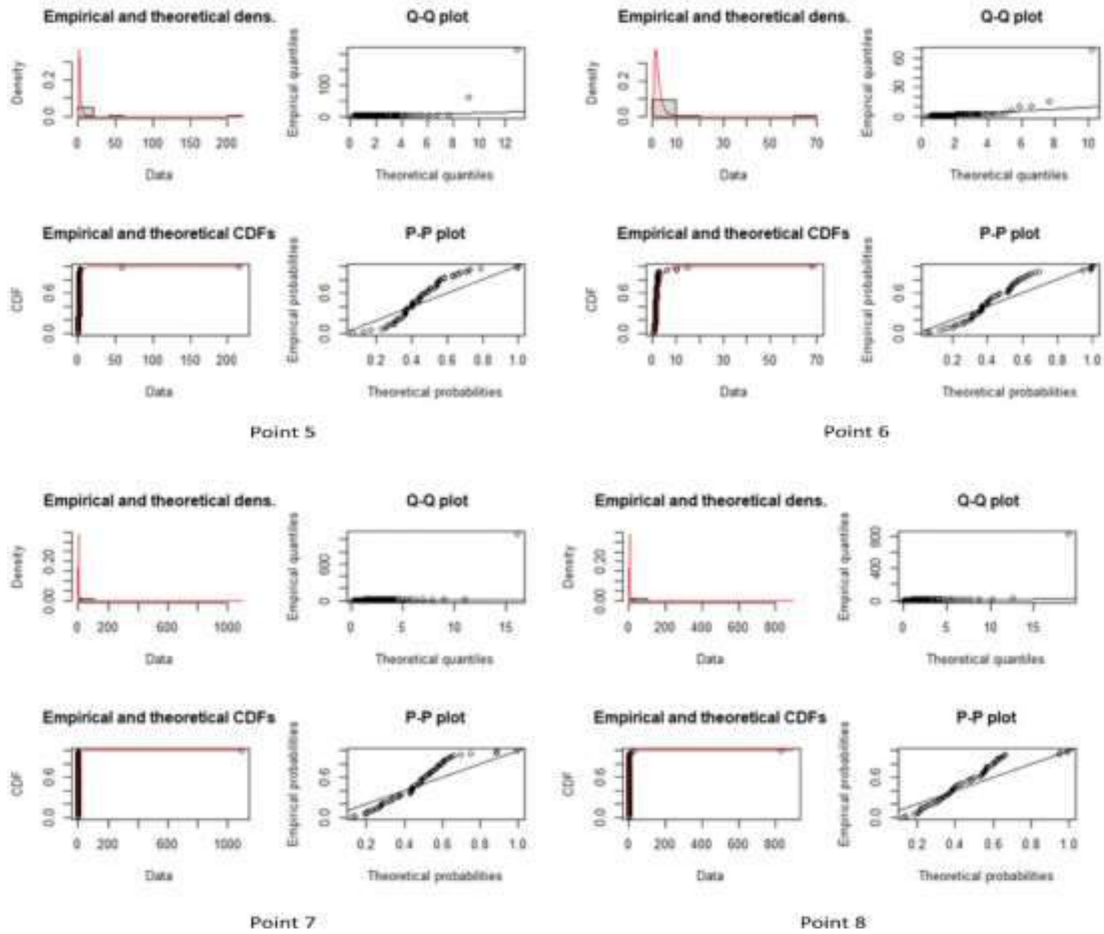

Figure 125. Theoretical probability density functions (PDFs) and the cumulative density functions (CDFs), applied as best-fit on the Chl-a data of points 5 - 8.

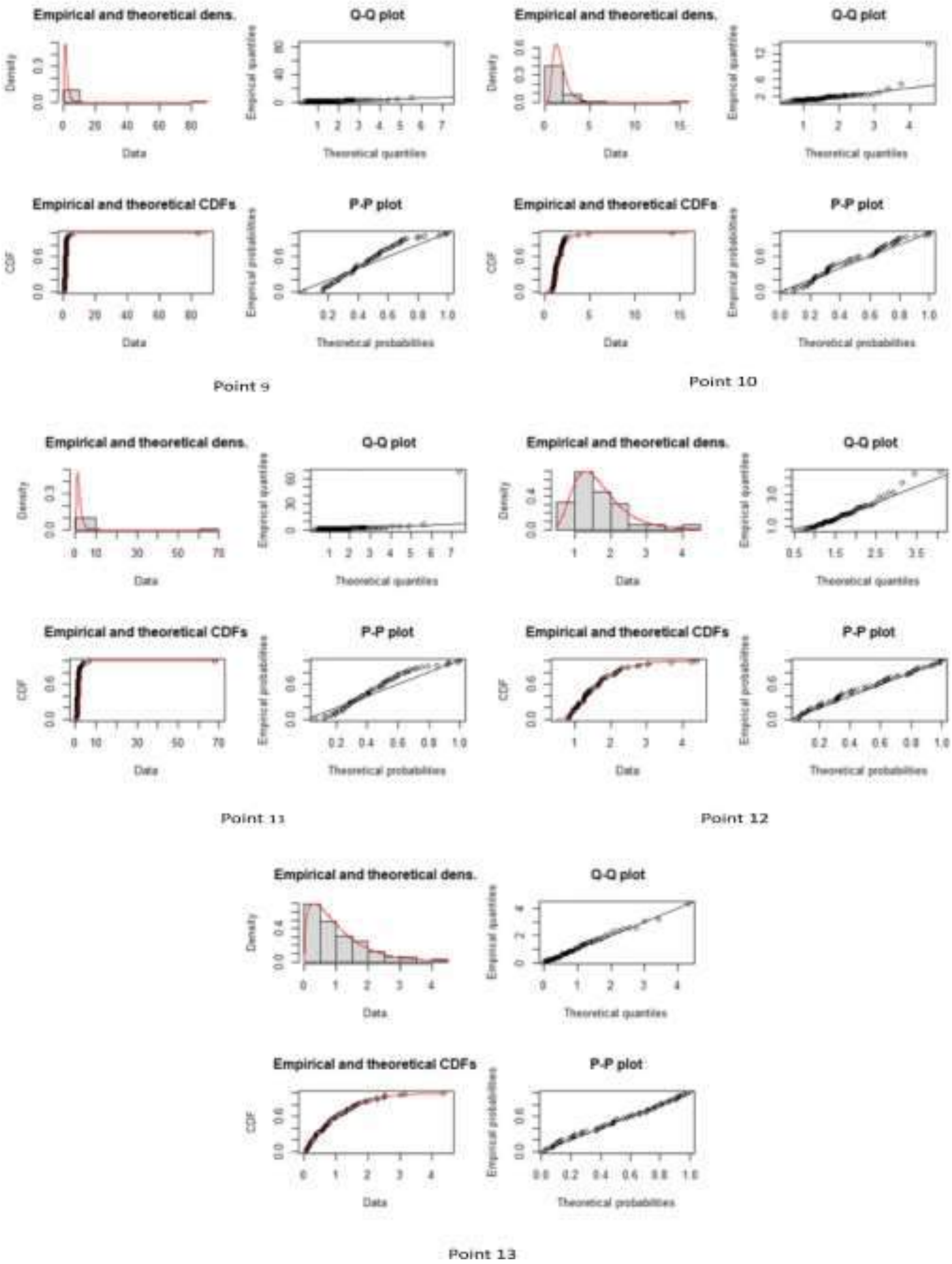

Figure 126. Theoretical probability density functions (PDFs) and the cumulative density functions (CDFs), applied as best-fit on the Chl-a data of points 9 – 13.

Based on the best-fit theoretical CDFs applied on the Chl-a, the probability of exceeding the eutrophication threshold of 2 μg/l was estimated. Probabilities of exceedance for all Porto Lagos lagoon points are summarized in Table 34. Probability is a measure that ranges between 0 and 1, with zero implying that eutrophication is impossible and 1 implying that eutrophication is absolutely certain. Figure 127 illustrates the probability map of exceedance of the eutrophication threshold in Porto Lagos lagoon.

Table 34. Probability of exceedance of the eutrophication threshold in Porto Lagos lagoon.

Points	Probability of Exceedance
1	0.436
2	0.517
3	0.290
4	0.330
5	0.460
6	0.491
7	0.468
8	0.478
9	0.352
10	0.269
11	0.362
12	0.258
13	0.133

Based on the above, points 1, 2, 5, 6, 7 and 8 are more vulnerable to eutrophication effects than the rest of the lagoon. These points are located at the north west basin of the lagoon. Exceedance probability is approx. 0.5, meaning that during half of a typical year eutrophication may exist. Based on the available Sentinel images, it seems that the eutrophication prone periods are spring and summer. On the contrary, points located at the east basin have limited probability for a eutrophication event.

Figure 127. Probability map of exceedance of the eutrophication threshold in Porto Lagos lagoon.

3.2.2.5 *Xirolimni*

The points selected for Chl-a concentration extraction for the eutrophication assessment in Xirolimni lagoon, are shown in Figure 95.

Table 35. Statistical measures per point for Chl-a concentration at Xirolimni Lagoon. presents the statistical measures for Chl-a concentration at all points examined in Xirolimni lagoon.

Table 35. Statistical measures per point for Chl-a concentration at Xirolimni Lagoon.

Points	Min	Max	Median	Mean	St. deviation	Skewness	Kurtosis
1	0.095	208.517	2.386	5.819	25.431	8.032	67.958
2	0.052	5.566	2.089	2.033	0.760	1.319	9.812
3	0.040	49.868	2.318	3.739	6.763	5.748	39.144
4	0.675	53.312	2.610	4.174	6.795	6.226	46.587
5	0.125	10.275	1.780	2.158	1.426	3.427	19.787
6	0.546	270.361	2.181	6.616	33.021	8.082	68.529
7	0.203	44.589	2.080	2.705	5.286	7.884	66.346

Figures 128 and 129 illustrate the skewness-kurtosis plot of Cullen and Frey for the Sentinel extracted Chl-a at all points in Xirolimni lagoon. Based on these graphs and the AIC and BIC criteria, it occurs that:

a) For Point 2, the normal distribution was found to be the best-fit theoretical distribution;
b) For Points 1, 3, 4, 6 and 7, the log-normal distribution was found to be the best-fit theoretical distribution;
c) For Point 5, the gumbel distribution was found to be the best-fit theoretical distribution.

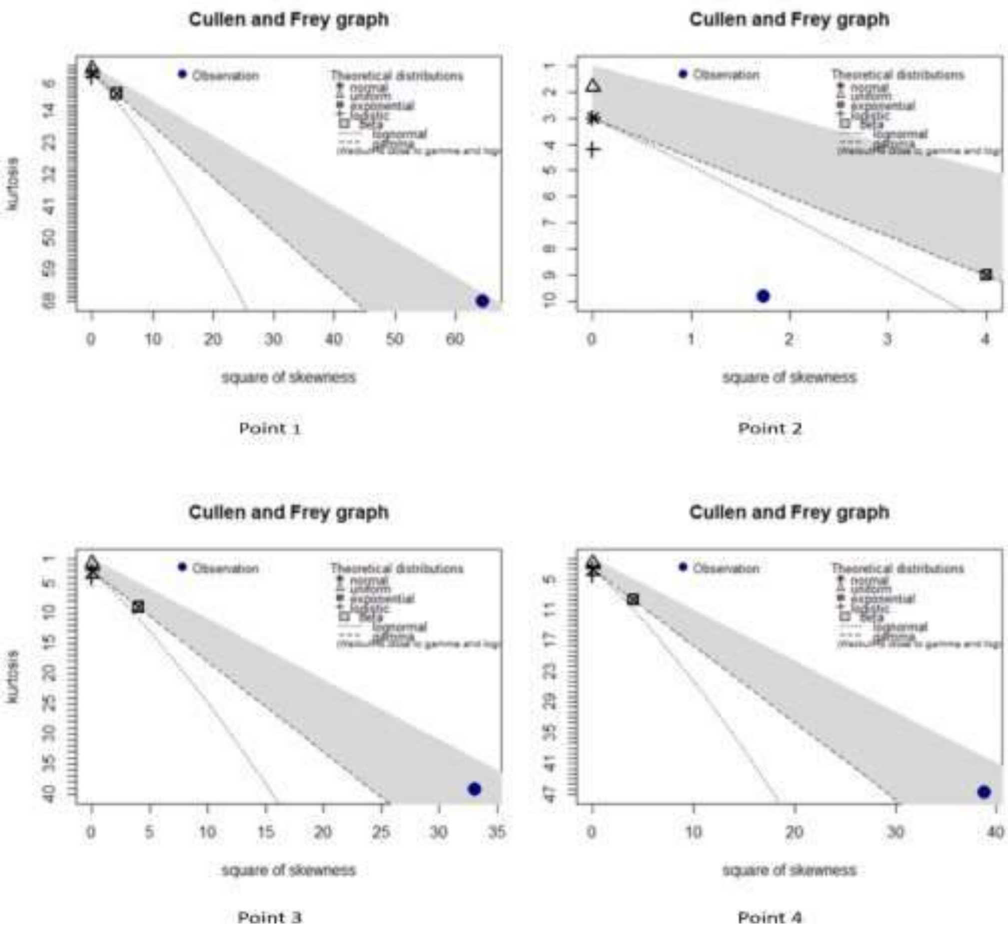

Figure 128. The Cullen and Frey diagrams for the distribution of Chl-a concentration at Points 1 - 4.

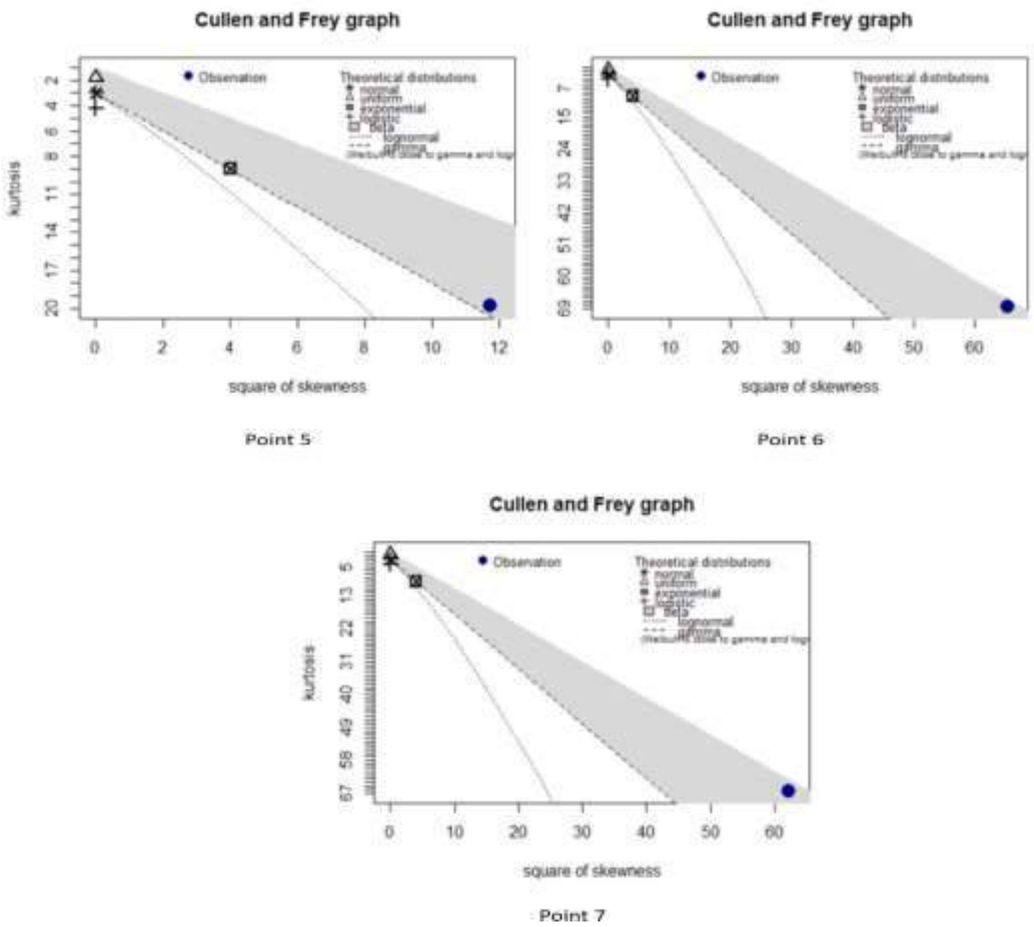

Figure 129. The Cullen and Frey diagrams for the distribution of Chl-a concentration at Points 5 - 7.

Table 36. Fitting parameters of the best-fit theoretical probability density function. presents the fitting parameters of the best-fit theoretical probability density function applied on the Chl-a concentration data extracted from Sentinel in Xirolimni lagoon. Mean and standard deviation parameters are given for the normal PDFs, log(mean) and log(sd) parameters for the log-normal distributions and shape and scale for the gamma distributions.

Table 36. Fitting parameters of the best-fit theoretical probability density function.

Points	**1**	**2**	**3**	**4**	**5**	**6**	**7**
Mean		2.033					
St Dev		0.754					
Log(Mean)	0.884		0.828	1.072		0.866	0.696
Log(St Dev)	0.100		0.115	0.084		0.094	0.071
Shape							
Scale							
a					1.645		
b					0.838		

LogLikelihood	-138.512	-75.002	-143.835	-139.018	-94.729	-133.074	-103.048
AIC	281.023	154.004	291.670	282.037	193.457	270.149	210.096
BIC	285.403	158.383	296.050	286.416	197.836	274.528	214.475

The theoretical probability density functions (PDFs) and the cumulative density functions (CDFs) applied as best-fit on the Chl-a data, together with the relevant Q-to-Q and P-to-P plots are shown in Figures 130 and 131.

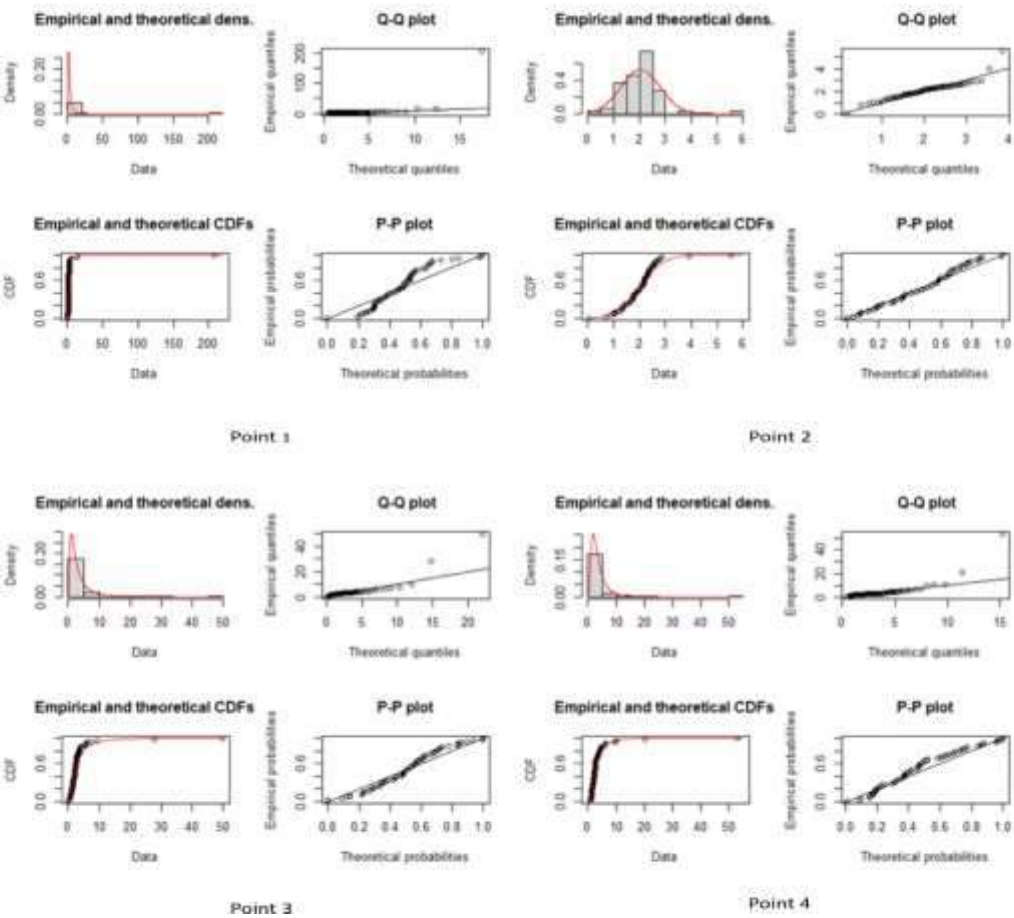

Figure 130. Theoretical probability density functions (PDFs) and the cumulative density functions (CDFs), applied as best-fit on the Chl-a data of points 1 – 4.

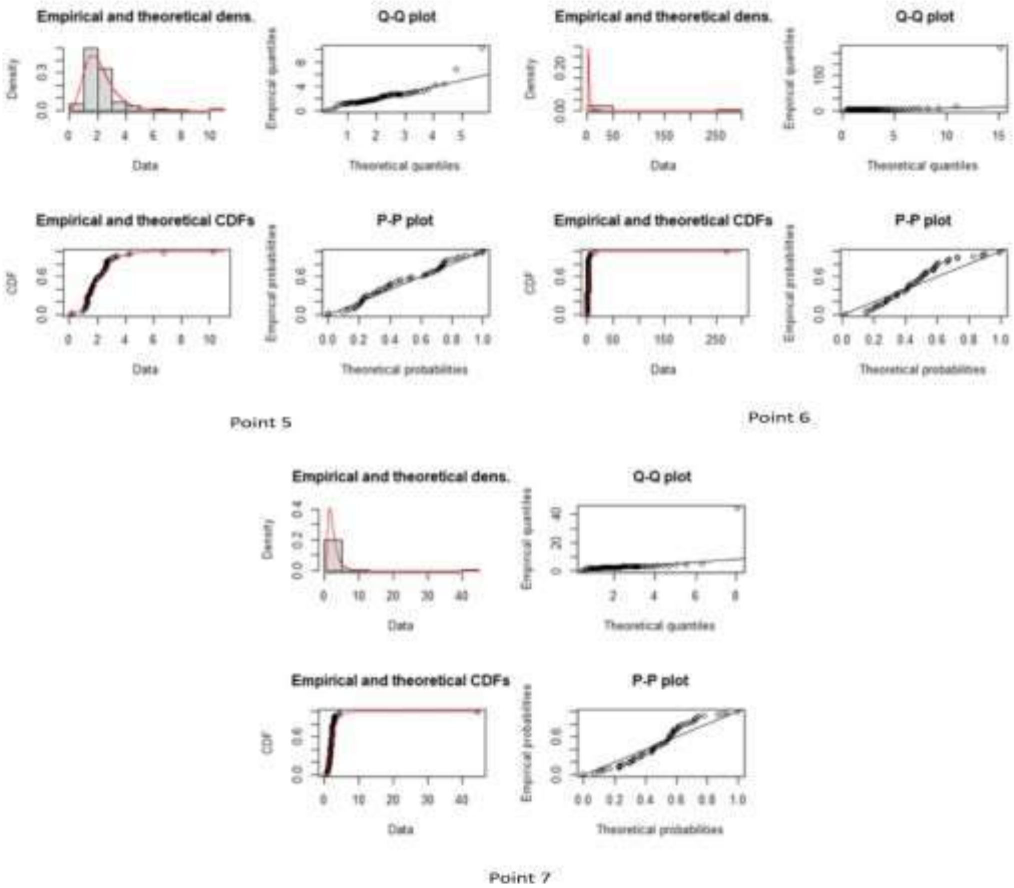

Figure 131. Theoretical probability density functions (PDFs) and the cumulative density functions (CDFs), applied as best-fit on the Chl-a data of points 5 – 7.

Based on the best-fit theoretical CDFs applied on the Chl-a, the probability of exceeding the eutrophication threshold of 2 μg/l was estimated. Probabilities of exceedance for all Xirolimni lagoon points are summarized in Table 37. Probability is a measure that ranges between 0 and 1, with zero implying that eutrophication is impossible and 1 implying that eutrophication is absolutely certain. Figure 132 illustrates the probability map of exceedance of the eutrophication threshold in Xirolimni lagoon.

Table 37. Probability of exceedance of the eutrophication threshold in Xirolimni lagoon.

Points	**Probability of Exceedance**
1	0.592
2	0.517
3	0.557
4	0.711
5	0.520
6	0.590
7	0.502

Based on the above, all points are vulnerable to eutrophication effects with exceedance probability over 0.5. Point 4, which is located on the southern part of the lagoon, shows the higher exceedance probability around 0.7. Based on the available Sentinel images, it seems that the eutrophication prone periods are spring and summer.

Figure 132. Probability map of exceedance of the eutrophication threshold in Xirolimni lagoon.

3.2.2.6 Ptelea

The points selected for Chl-a concentration extraction for the eutrophication assessment in Ptelea lagoon, are shown in Figure 101.

Table 38 presents the statistical measures for Chl-a concentration at all points examined in Ptelea lagoon.

Table 38. Statistical measures per point for Chl-a concentration at Ptelea Lagoon.

Points	Min	Max	Median	Mean	St. deviation	Skewness	Kurtosis
1	0.597	93.855	5.998	12.938	17.527	2.764	11.892
2	0.010	53.320	6.087	10.710	12.002	2.063	6.722
3	0.085	6.881	1.549	1.689	1.082	1.802	9.787
4	0.340	225.318	5.768	15.535	29.925	5.558	40.297

5	0.083	242.107	5.467	15.358	32.397	5.732	40.858
6	0.535	285.309	9.329	27.705	55.905	3.437	14.903

Figures 133 and 134 illustrate the skewness-kurtosis plot of Cullen and Frey for the Sentinel extracted Chl-a at all points in Ptelea lagoon. Based on these graphs and the AIC and BIC criteria, it occurs that:

a) For Points 1, 4, 5 and 6, the log-normal distribution was found to be the best-fit theoretical distribution;
b) For Point 3, the gamma distribution was found to be the best-fit theoretical distribution;
c) For Point 2, the gumbel distribution was found to be the best-fit theoretical distribution;

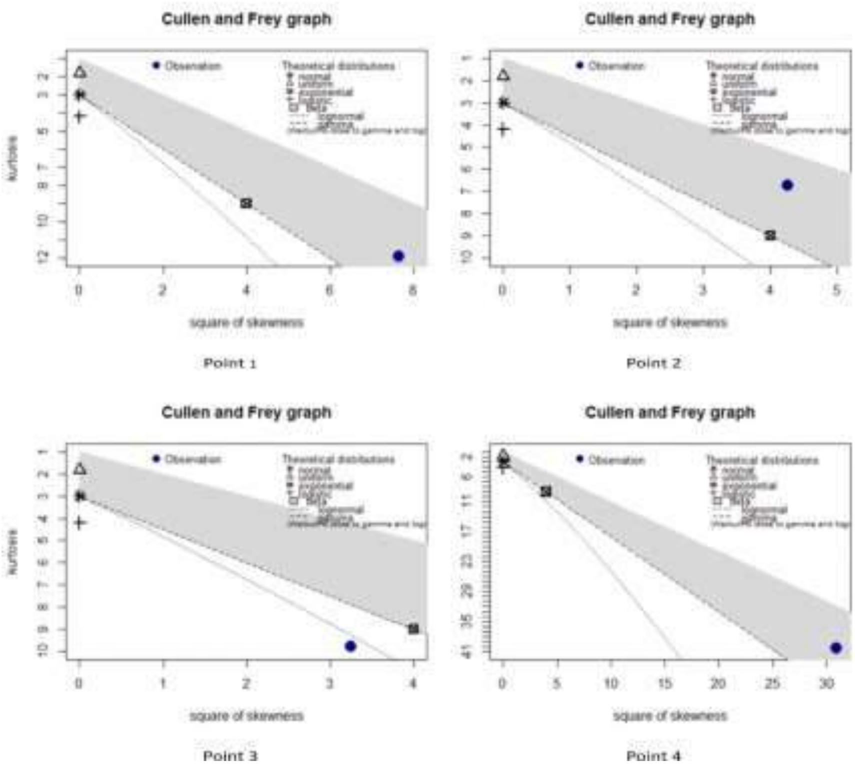

Figure 133. The Cullen and Frey diagrams for the distribution of Chl-a concentration at Points 1 - 4.

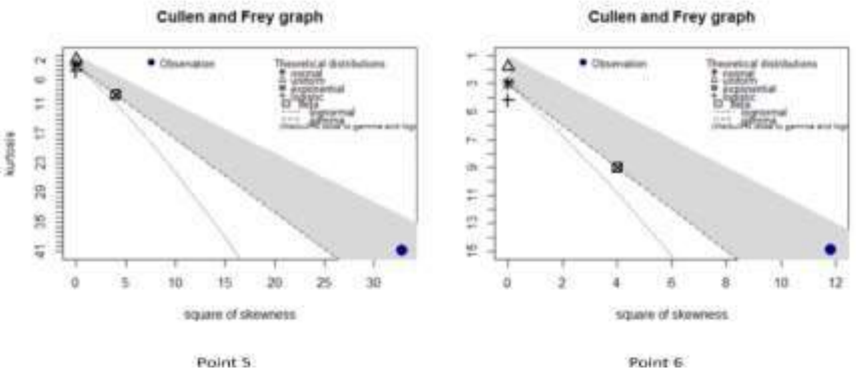

Figure 134. The Cullen and Frey diagrams for the distribution of Chl-a concentration at Points 5 - 6.

Table 39 presents the fitting parameters of the best-fit theoretical probability density function applied on the Chl-a concentration data extracted from Sentinel in Ptelea lagoon. Mean and standard deviation parameters are given for the normal PDFs, log(mean) and log(sd) parameters for the log-normal distributions and shape and scale for the gamma distributions.

Table 39. Fitting parameters of the best-fit theoretical probability density function.

Points	1	2	3	4	5	6
Mean						
St Dev						
Log(Mean)	1.927			1.964	1.938	2.364
Log(St Dev)	0.135			0.147	0.147	0.150
Shape			1.647			
Scale						
a		6.196				
b		6.292				
LogLikelihood	-230.642	-238.302	-90.760	-239.017	-237.374	-267.301
AIC	465.284	480.605	185.521	482.034	478.747	538.603
BIC	469.694	485.014	189.930	486.443	483.157	543.012

The theoretical probability density functions (PDFs) and the cumulative density functions (CDFs) applied as best-fit on the Chl-a data, together with the relevant Q-to-Q and P-to-P plots are shown in Figures 135 and 136.

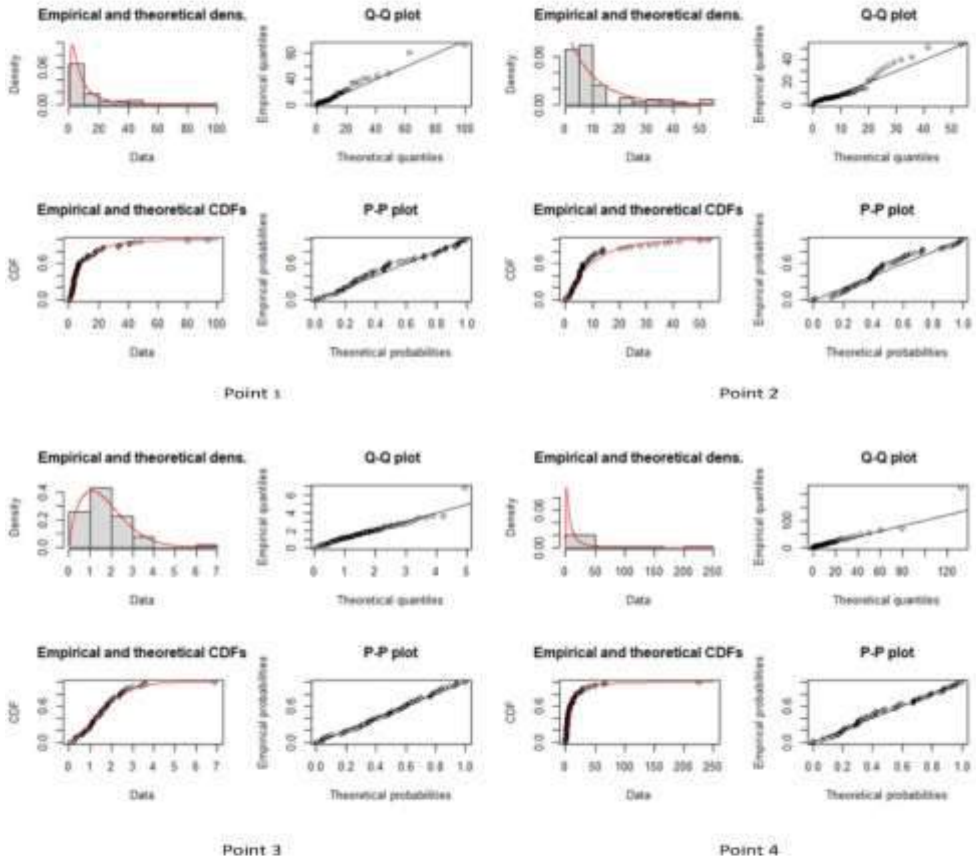

Figure 135. Theoretical probability density functions (PDFs) and the cumulative density functions (CDFs), applied as best-fit on the Chl-a data of points 1 – 4.

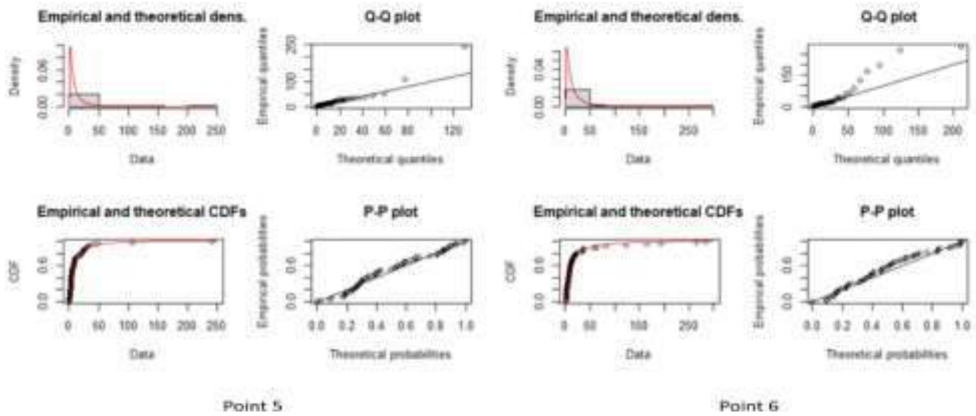

Figure 136. Theoretical probability density functions (PDFs) and the cumulative density functions (CDFs), applied as best-fit on the Chl-a data of points 5 – 6.

Based on the best-fit theoretical CDFs applied on the Chl-a, the probability of exceeding the eutrophication threshold of 2 μg/l was estimated. Probabilities of exceedance for all Ptelea lagoon points are summarized in Table 40. Probability is a measure that ranges between 0 and 1, with zero implying that eutrophication is impossible and 1 implying that eutrophication is absolutely certain. Figure 137 illustrates the probability map of exceedance of the eutrophication threshold in Ptelea lagoon.

Table 40. Probability of exceedance of the eutrophication threshold in Ptelea lagoon.

Points	Probability of Exceedance
1	0.869
2	0.824
3	0.686
4	0.855
5	0.849
6	0.913

Based on the above, all points are vulnerable to eutrophication effects. Exceedance probability varies from 0.7 to 0.9, meaning there is high probability eutrophication may exist during a typical year. Based on the available Sentinel images, it seems that the eutrophication prone periods are spring and summer.

Figure 137. Probability map of exceedance of the eutrophication threshold in Ptelea lagoon.

4 Conclusions

In this work, a neuro-fuzzy model was developed to estimate Chl-a values from Landsat 8 and Sentinel-2 satellite images. The model was trained using in-situ data collected at times coinciding to the crossing of these satellites. The model was implemented at the reflectance data from 6 lagoons of the Nestos and Vistonis complexes in Northern Greece.

The annual evolution of Chl-a in Vassova lagoon registers two maxima. The first one occurs in spring (May-June) and the next one in the summer around August. The center of the lagoon and the north part are the parts that usually show higher Chl-a values than the rest of the basin.

Eratino and Agiasma exhibit three peaks, one in spring (April-May), the second one in summer and the third one in November. In Eratino, higher Chl-a values occur at the center and the southeast parts and in Agiasma at the northern part.

In Porto Lagos, higher Chl-a values occur at the northern part and the southeast basin. Throughout the years studied, a regular peak was recorded around July-August.

In Xirolimni lagoon, the first peak occurs in late spring, and the second one in November and Chl-a was found to be in greater concentration across the shores.

Finally, Ptelea shows higher Chl-a concentration values compared to the other lagoons studied. Chl-a values determined range from 1.0 to 40.0 μg/l, while the values in the other lagoons rarely exceed 5 μg/l.

5 References

Antoine, D., André, J.-M., Morel, A., 1996. Oceanic primary production: 2. Estimation at global scale from satellite (Coastal Zone Color Scanner) chlorophyll. Global Biogeochemical Cycles 10, 57-69.

Brezonik, P., Menken, K.D., Bauer, M., 2005. Landsat-based Remote Sensing of Lake Water Quality Characteristics, Including Chlorophyll and Colored Dissolved Organic Matter (CDOM). Lake and Reservoir Management 21, 373-382.

Bukata, R.P., 2013. Retrospection and introspection on remote sensing of inland water quality:"Like Déjà Vu All Over Again". Journal of Great Lakes Research, 2-5.

Cao, Z., Ma, R., Duan, H., Pahlevan, N., Melack, J., Shen, M., Xue, K., 2020. A machine learning approach to estimate chlorophyll-a from Landsat-8 measurements in inland lakes. Remote Sensing of Environment 248, 111974.

Costanza, R., d'Arge, R., de Groot, R., Farber, S., Grasso, M., Hannon, B., Limburg, K., Naeem, S., O'Neill, R.V., Paruelo, J., Raskin, R.G., Sutton, P., van den Belt, M., 1997. The value of the world's ecosystem services and natural capital. Nature 387, 253-260.

Cullen, A.C., Frey, H.C., 1999. Probabilistic techniques in exposure assessment. Plenum Press, USA, pp. 81-159.

Dall'Olmo, G., Gitelson, A., Rundquist, D., Leavitt, B., Barrow, T., Holz, J., 2005. Assessing the potential of SeaWiFS and MODIS for estimating chlorophyll concentration in turbid productive waters using red and near-infrared bands. Remote Sensing of Environment 96, 176-187.

Devlin, M., Bricker, S., Painting, S., 2011. Comparison of five methods for assessing impacts of nutrient enrichment using estuarine case studies. Biogeochemistry 106, 177-205.

Gholizadeh, M.H., Melesse, A.M., Reddi, L., 2016. A Comprehensive Review on Water Quality Parameters Estimation Using Remote Sensing Techniques. Sensors 16.

Gitelson, A., Dall'Olmo, G., Moses, W., Rundquist, D., Barrow, T., Fisher, T., Gurlin, D., Holz, J., 2008. A Simple semi-analytical model for remote estimation of chlorophyll-a in turbid waters: Validation. Remote Sensing of Environment 112, 3582-3593.

Gurlin, D., Gitelson, A.A., Moses, W.J., 2011. Remote estimation of chl-a concentration in turbid productive waters — Return to a simple two-band NIR-red model? Remote sensing of environment. 115, 3479-3490.

Han, L., 1997. Spectral reflectance with varying suspended sediment concentrations in clear and algae-laden waters. Photogrammetric engineering and remote sensing 63, 701-705.

Han, L., Jordan, K.J., 2005. Estimating and mapping chlorophyll-a concentration in Pensacola Bay, Florida using Landsat ETM+ data. International Journal of Remote Sensing 26, 5245-5254.

Hu, C., Lee, Z., Franz, B., 2012. Chlorophyll aalgorithms for oligotrophic oceans: A novel approach based on three-band reflectance difference. Journal of Geophysical Research: Oceans 117.

Ibelings, B.W., Vonk, M., Los, H.F.J., van der Molen, D.T., Mooij, W.M., 2003. FUZZY MODELING OF CYANOBACTERIAL SURFACE WATERBLOOMS: VALIDATION WITH NOAA-AVHRR SATELLITE IMAGES. Ecological Applications 13, 1456-1472.

Jimeno-Sáez, P., Senent-Aparicio, J., Cecilia, J.M., Pérez-Sánchez, J., 2020. Using Machine-Learning Algorithms for Eutrophication Modeling: Case Study of Mar Menor Lagoon (Spain). 17, 1189.

Jordan, T.E., Correll, D.L., Miklas, J.J., Weller, D.E., 1991. Long-term trends in estuarine nutrients and chlorophyll, and short-term effects of variation in watershed discharge. Marine Ecology Progress Series.

Kadiri, M., Zhang, H., Angeloudis, A., Piggott, M.D., 2021. Evaluating the eutrophication risk of an artificial tidal lagoon. Ocean & Coastal Management 203, 105490.

Karydis, M., 1996. Quantitative assessment of eutrophication: A scoring system for characterising water quality in coastal marine ecosystems. Environmental Monitoring and Assessment 41, 233-246.

Kirk, J.T.O., 1994. Light and photosynthesis in aquatic ecosystems. Cambridge university press.

Kjerfve, B., 1994. Coastal lagoon processes. Elsevier.

Koutrakis, E., Emfietzis, G., Sylaios, G., Zoidou, M., Katsiapi, M., Moustaka-Gouni, M.J.M.M.S., 2016. MASSIVE FISH MORTALITY IN ISMARIDA LAKE, GREECE: IDENTIFICATION OF DRIVERS CONTRIBUTING TO THE FISH KILL EVENT. 17, 280-291.

Koutrakis, E.T., Tsikliras, A.C., Sinis, A.I., 2005. Temporal variability of the ichthyofauna in a Northern Aegean coastal lagoon (Greece). Influence of environmental factors. Hydrobiologia 543, 245-257.

Liu, G., Li, L., Song, K., Li, Y., Lyu, H., Wen, Z., Fang, C., Bi, S., Sun, X., Wang, Z., Cao, Z., Shang, Y., Yu, G., Zheng, Z., Huang, C., Xu, Y., Shi, K., 2020. An OLCI-based algorithm for semi-empirically partitioning absorption coefficient and estimating chlorophyll a concentration in various turbid case-2 waters. Remote Sensing of Environment 239, 111648.

Mobley, C.D., 1995. The optical properties of water. Handbook of optics 1, 43-43.

Morrow, J.H., White, B.N., Chimiente, M., Hubler, S., 2000. A bio-optical approach to reservoir monitoring in Los Angeles, California. Advances in limnology. Stuttgart, 179-191.

O'Reilly, J.E., Maritorena, S., Mitchell, B.G., Siegel, D.A., Carder, K.L., Garver, S.A., Kahru, M., McClain, C., 1998. Ocean color chlorophyll algorithms for SeaWiFS. Journal of Geophysical Research: Oceans 103, 24937-24953.

Ogashawara, I., Moreno-Madriñán, M.J., 2014. Improving inland water quality monitoring through remote sensing techniques. ISPRS International Journal of Geo-Information 3, 1234-1255.

Orfanidis, S., Pinna, M., Sabetta, L., Stamatis, N., Nakou, K., 2008. Variation of structural and functional metrics in macrophyte communities within two habitats of eastern Mediterranean coastal lagoons: natural versus human effects. Aquatic Conservation: Marine and Freshwater Ecosystems 18, S45-S61.

Ouma, Y.O., Noor, K., Herbert, K., 2020. Modelling Reservoir Chlorophyll-<i>a</i>, TSS, and Turbidity Using Sentinel-2A MSI and Landsat-8 OLI Satellite Sensors with Empirical Multivariate Regression. Journal of Sensors 2020, 8858408.

Palmer, S.C.J., Kutser, T., Hunter, P.D., 2015. Remote sensing of inland waters: Challenges, progress and future directions. Elsevier.

Schalles, J.F., 2006. OPTICAL REMOTE SENSING TECHNIQUES TO ESTIMATE PHYTOPLANKTON CHLOROPHYLL a CONCENTRATIONS IN COASTAL, in: Richardson, L.L., LeDrew, E.F. (Eds.), Remote sensing of aquatic coastal ecosystem processes. Springer Netherlands, Dordrecht, pp. 27-79.

Shumway, S.E., 1990. A Review of the Effects of Algal Blooms on Shellfish and Aquaculture. 21, 65-104.

Simboura, N., Panayotidis, P., Papathanassiou, E., 2005. A synthesis of the biological quality elements for the implementation of the European Water Framework Directive in the Mediterranean ecoregion: The case of Saronikos Gulf. Ecological Indicators 5, 253-266.

Sylaios, G., Theocharis, V., 2002. Hydrology and nutrient enrichment at two coastal lagoon systems in Northern Greece. Water Resources Management 16, 171-196.

Sylaios, G.K., Tsihrintzis, V.A., Akratos, C., Haralambidou, K., 2006. Quantification of water, salt and nutrient exchange processes at the mouth of a Mediterranean coastal lagoon. Environmental monitoring and assessment 119, 275-301.

Toming, K., Kutser, T., Laas, A., Sepp, M., Paavel, B., Nõges, T., 2016. First Experiences in Mapping Lake Water Quality Parameters with Sentinel-2 MSI Imagery. 8, 640.

Tsihrintzis, V., Sylaios, G., Sidiropoulou, M., Koutrakis, E., 2007. Hydrodynamic modeling and management alternatives in a Mediterranean, fishery exploited, coastal lagoon. Aquacultural Engineering 36, 310-324.

Yew-Hoong Gin, K., Teck Koh, S., Lin, I.I., Soon Chan, E., 2002. Application of Spectral Signatures and Colour Ratios to Estimate Chlorophyll in Singapore's Coastal Waters. Estuarine, Coastal and Shelf Science 55, 719-728.

Zanchettin, D., Traverso, P., Tomasino, M.J.H., 2007. Observations on future sea level changes in the Venice lagoon. 577, 41-53.